May 2018

Transient Load Recovery Using Strain Measurements and Model Reduction

Bibek Wagle
University of Wisconsin-Milwaukee

TRANSIENT LOAD RECOVERY USING STRAIN MEASUREMENTS AND MODEL REDUCTION

by

Bibek Wagle

A Thesis Submitted in

Partial Fulfilment of the

Requirements for the Degree of

Master of Science

in Engineering

at

The University of Wisconsin – Milwaukee

May 2018

ABSTRACT

TRANSIENT LOAD RECOVERY USING STRAIN MEASUREMENTS AND MODEL REDUCTION

by

Bibek Wagle

The University of Wisconsin - Milwaukee, 2018
Under the Supervision of Professor Anoop K. Dhingra

A transient load is defined as a loading condition where the magnitude of the load changes rapidly in a short period of time. Impact loads are a common example of transient loading. It is well known that impact loads can have disastrous effect on the structure compared loads applied over a longer period of time. An identification of impact loads is an important aspect in the design of structures.

A direct identification of applied force on a structure through use of force transducers is not possible under all situations. In such cases, the structural response could be used to recover the imposed loading. Various structural responses such as displacement, stress or strain could be used to recover the imposed loads. However, this thesis focuses on a use of strain data to recover impact loads acting on a component.

The strain data is extracted by placing strain gages at different locations on the component. A selection of the location for strain gages is tricky because the accuracy of the load recovery is sensitive to the position of the sensors. A D-optimal technique is used in this thesis to determine the optimum location of sensors so that most accurate results for load estimates are obtained. With sensors placed at the optimum locations, the strain data was extracted. The

extracted strain data was used in conjunction with component's modal data to approximate mode participation factors. The approximated mode participation factors and displacement mode shapes were next used to approximate displacements, velocities and accelerations. Finally, this information was used to estimate the loads acting on the component.

A drawback of this approach is that it requires modal information of the entire structure be available. However, practical computational considerations limit the use of information of all modes. To overcome this difficulty, reduced order modeling based on Craig-Bampton model reduction is used. It is seen that Craig-Bampton reduction allows for an accurate estimation of imposed loads while utilizing only a small subset of available modal information.

Dedicated to my Parents Bishnu Prasad Wagle and Bed Kumari Wagle,

For their imperishable love, dedication and motivation

TABLE OF CONTENTS

LIST OF FIGURES

LIST OF TABLES

ACKNOWLEDGEMENTS

Initially, I would like to sincerely thank my advisor Dr. Anoop Dhingra for providing me an excellent opportunity to work on this research under his guidance. Without his valuable time, effort, suggestions and recommendations, this research would have been impossible. Secondly, I would also like to thank my committee members Professors Michael Nosonovsky and Ben Church for providing valuable suggestions and recommendations.

I would also like to thank my colleagues SK Hasan, Bella Jackson, Hana Alqam and Hussain Altammar for providing a friendly work environment and providing their valuable input and suggestion on the research.

I am also grateful to my family in Nepal for their continuous moral support. Finally, I am thankful to my Uncle Ramnath Pokharel and Aunt Bimala Kaphle for providing a homely environment in Milwaukee, Wisconsin.

1 Introduction

1.1 Problem Statement

For reliable and cost effective design of structure or equipment, prior information about locations and magnitudes of the external loads transmitted to the structure is desirable. These loads may be static, transient or impact loads. Since the stresses and strains induced in the structure are a function of the imposed loads, prior knowledge of the loads in the design process is crucial for design optimization. Accurate prediction of loads early in the design process will facilitate a reliable and cost effective design of the structure.

1.2 Limitation of load transducers

Normally, direct measurement of loads through force transducer is feasible for it involves inserting a load transducer between the structure and the load transferring body. However, this method has drawbacks and suffers from limitations. Installation of load transducer might change the dynamic characteristic of the system leading to inaccurate load estimation. Also, the point of the load location might be difficult to access and installation of load transducer might not be possible. Direct measurement of the excitation loads is also not feasible in many case such as those involving distributed loadings such as wind load, seismic excitation and fluid-flow induced force.

1.3 Using structure as a load transducer

In many cases, the structure itself could be used as load transducer. Structural response like displacement, acceleration, stresses and strains are also direct function of applied excitation loads. The relationship between induced structural response and excitation load could be used to identify the loads. However, solving this problem is not easy as it seems. Though the forward problem i.e. where excitation force and location is given and structural response to be

determined, is easy and straight forward, the inverse problem i.e. where structural response is given and force needs to be identified, is difficult and complex because the solution might not be unique. Further, inverse problems generally tend to be quite ill-conditioned numerically. This research presents one of such methods to identify impact force loading using inverse methods.

1.4 Organization of the Material

Chapter 1 of the thesis provides introduction of the overall research. It clearly states the problem statement and solution methodology. It also provides an overview of the material covered in each chapter.

Chapter 2 provides information about the research done previously in the field. It also discusses methodologies, shortcomings, scope of improvement on previous efforts and presents a new approach to estimate impact loads.

Chapter 3 covers about the recovery of static and quasi-static load using strain measurements. It presents an example of a flat plate and bent cantilever beam and describes the algorithm for load recovery using strain measurements.

Chapter 4 discusses transient load recovery using strain measurements. Strain at optimum gage location are extracted and strain values are used to calculate mode participation factors. The displacement mode shapes are also extracted and displacement and acceleration are calculated using mode participation factor and mode shapes. The Craig-Bampton reduction is technique is used to reduce size of the computational model. This chapter also paves a way and provides an algorithm that can be used to recover transient loads.

Chapter 5 discusses impact load recovery using strain measurements. The same algorithm that was used in chapter 4 is used to recover impact loads. Three type of impact loading,

triangular wave loading, square wave loading and half-sine wave loading are applied on a flat plate and the impact loads were recovered using Craig-Bampton reduction technique.

Chapter 6 presents a summary of the work done throughout the research. It also outlines scope of the future research that can be used to extend the method presented in this thesis.

2 Literature Review

Over the past many years, several researchers have addressed the problem to identify the loads on structure. Normally identification of these loads becomes difficult because direct measurement through force transducer is not possible or extremely difficult. In such cases, force identification through inverse technique is a feasible option. Impact load identification is one of the important field because sudden impact load might cause catastrophic effects. The breakup of space shuttle Columbia during reentry in 2003 was one of those deadly catastrophic effect caused by impact loading. So, scientists and engineers have been intensively researching the effects of impact loading on the component and how to estimate the magnitude of impact loads. Similar attempt is done in this thesis to identify the impact loading. In this chapter, a review of the research done in this field is briefly explained.

2.1 Static Load Identification

Static load is defined as load condition where the load does not vary with time. This the simplest form of loading. In a simple structure, static load might by easily identified by using the simple mathematical formula given that the required data are known. However, things are more cumbersome in a complex structure. Computer simulated finite element modelling drastically reduces the complexity of the problem, however, a smart algorithm needs to be applied to recover the load. Data extracted from strain gage placement at certain location and their identification through inverse methods is one of such feasible option.

Masroor and Zachary (1991) developed a technique to determine the load applied to a component by using the strain data. However, the placement of strain gages in their approach was random and did not guarantee optimal placement of gages. Though they tried different sets

of possible strain gauge placements, their selection does not guarantee that gages are placed at optimal location, hence, the solution approach might not yield the best possible load estimates.

Wickham et al. (1995) developed smart algorithm utilizing k-exchange algorithm proposed by Johnson and Nachtsheim (1983) to construct the D-optimal design to estimate the loads. This technique is fairly effective and the same technique will be applied in this research to mount the strain gages.

2.2 Impact load identification

`

Impact load is a large force or shock applied over short period of time. Usually impact loads cause a greater damage than a lower magnitude force applied over a proportionally longer period of time. Considering the disastrous effect of impulse excitation force on the structure, impact load identification has become the subject of several studies. Ma ,Chih-Kao, et al. (1998) proposed a technique by applying Kalman filter with recursive estimator to determine impulsive loads. The impulsive loads were estimated form the measured dynamic response data of structure through inverse methods by using a least-square algorithm.

Hillary and Ewins (1984) tested a cantilever beam by using two sinusoidal forces of same frequency but different magnitudes. Their research showed poor results that were caused by contamination of the measurement noises.

Khoo et al. (2014) used a pseudo-inverse method on light weight structure for under-determined, even-determined and over determined cases. Their research noted that in the over-determined case, good combination of response and high number of response location gives the best accuracy of force identification result compared to under-determined and even determined case. Their research concluded that load could be pretty accurately estimated in case of over-determined problem and even-determined case when good locations were selected in advance.

However, their approach was unable to determine the force information in case of under-determined case.

2.3 Summary

Though a lot of research has taken place in the field of transient load identification, there are issues that needs to be addressed to improve computational efficiency, accuracy and real-world applications. It was noted that the load estimates were either contaminated with measurement noises or lacked smart algorithm to select optimum location of sensors. Majority of the transient and impact load identification techniques clearly lack the domain of optimum sensor location identification. Most of the researchers placed their sensors randomly or some ad-hoc locations based on prior knowledge of good locations. Because of this, the load estimates are either poor or prone to measurement noise. It was inferred from the previous research that the precision of load estimates is determined by the location of sensor placement. This thesis attempts to improve load estimates by using sensor data at locations that are determined optimally.

3 Static and Quasi-Static Load Recovery Using Strain Measurements

Measurements of strains at optimum locations of strain gages and using these measurements to recover the loads acting on the structure by inverse analysis has been used over the years. As compared to other types of structural response such as displacements, velocities or accelerations, strain gages provide one of the most inexpensive, robust and reliable method to estimate the applied loads. This chapter presents an in-depth investigation of the recovery of static loads and quasi static loads using strain measurements. Sec. 3.1 introduces theoretical background and procedure of load estimation process. Sec. 3.2 provides example of static load recovery on flat plate with a hole. Sec. 3.3 builds upon the concepts presented in Sec. 3.1 and explains quasi-static load recovery on a 3D cantilever beam.

3.1 Theoretical development

3.1.1 Design of Structure

The first process in the recovery of any load is to model the component on which the load is imposed. A model of the structure is created in ANSYS APDL. Appropriate meshing is done on the structure to generate finite elements such that the size of the element is compatible with size of the strain gages that could be mounted on the component.

3.1.2 Determination of Optimum Location

Out of the numerous elements on the structure, a specific set of elements is required to mount the strain gauges. For practical application, the number and location of strain gauges is usually determined by the budget, feasibility to mount the gages and their effect on the structural response.

3.1.2.1 Candidate set

The candidate set is defined as the all possible locations where a potential strain gage could be mounted. For purposes of our research, all the elements except points of force application are assumed to be candidate set. However, in practice, the candidate set might be limited since it's not practically feasible to mount gages in all locations. Out of the all possible locations in the candidate set, optimum locations are chosen to mount the gages. To pick the optimum locations, a special algorithm is implemented which is described in the section below.

3.1.2.2 Mohr's transformation

To pick the optimum set of sensor locations out of the candidate set, initially, a unit load is applied in each direction. The strain data for load cases is then extracted from ANSYS and imported in MATLAB. Since the goal of the research is not only to find the optimum gage locations but also the optimum angular orientation of each strain gage, the strains data extracted from MATLAB are transformed in 18 directions using Mohr's Transformation.

Mohr's transformation transforms the strain data extracted form ANSYS from a gage angle of 0 to 170 degrees in 10-degree increments. The strain matrix is created first which is given by,

$$strain = \begin{bmatrix} \varepsilon_x & \varepsilon_{xy}/2 & \varepsilon_{xz}/2 \\ \varepsilon_{xy}/2 & \varepsilon_y & \varepsilon_{yz}/2 \\ \varepsilon_{xz}/2 & \varepsilon_{yz}/2 & \varepsilon_z \end{bmatrix} \tag{3.1}$$

Since the Z-axis of each element is normal to the element, the strain data is transformed by considering rotations about the Z-axis using the matrix below:

$$T = \begin{bmatrix} \cos\theta & \sin\theta & 0 \\ -\sin\theta & \cos\theta & 0 \\ 0 & 0 & 1 \end{bmatrix} \tag{3.2}$$

where θ is corresponding angle measured counter-clockwise with respect to X-axis. Finally, the matrix of strains is transformed as

$$T_m = T * strain * T^T \qquad (3.3)$$

After the transformation is done, the number of entries candidate set will increase by 18 times. All the strain vectors corresponding to the transformed angles will be processed D-optimal design algorithm to pick the optimum locations and orientations.

3.1.2.3 D-optimal design algorithm

D-optimal design algorithm described below is used to find the optimum locations and orientations of strain gages. The algorithm consists of following steps.

a) At first, number of gages (g) to be mounted on the structure is specified.

b) Next, matrix A is created by randomly picking g-number of candidate point from the candidate set.

c) Matrix $A+$ is created by picking another row which is not already part of Matrix A such that the determinant of $|A+^T * A +|$ is maximized.

d) Next the matrix $A-^T * A -$ is formed by deleting a row from A+ such that the determinant is maximum.

e) The ratio of $|A-^T * A -|$ to $|A^T * A|$ is calculated till the ratio converges to 1 i.e. until there is no improvement is found and the process (c) to (e) is repeated till the ratio converges to 1 and the $A-$ matrix becomes the A matrix for the next iteration. Upon convergence, $A-$ will contain optimum sensor locations.

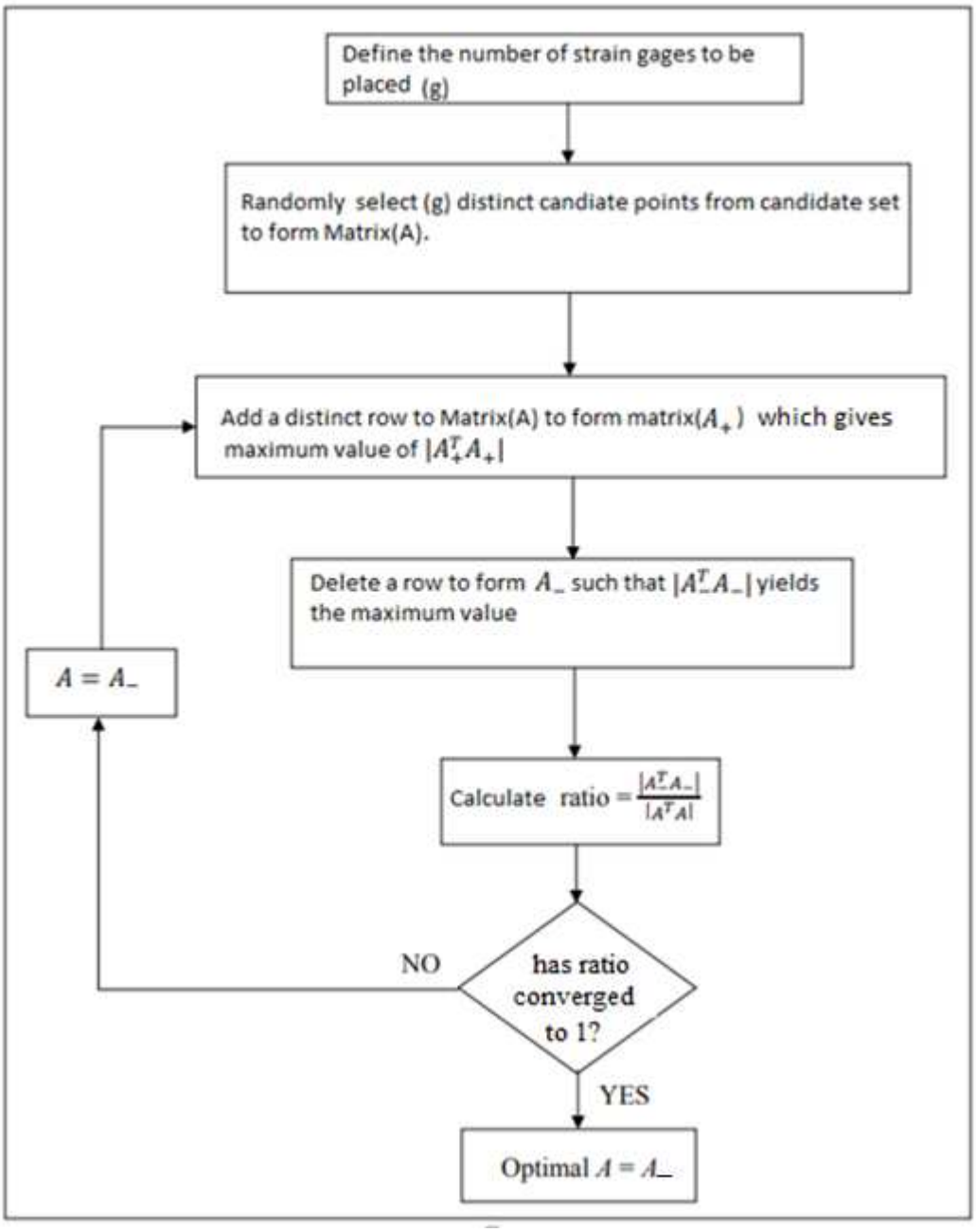

Figure 3.1: Flow chart of Sequential Exchange Algorithm

3.1.3 Strain Gauge Placement, Data extraction and Recovery

After the optimum gage locations and orientations are determined strain gages are placed at optimum locations. The strains are extracted and Mohr's transformation is done on the strain data corresponding to optimum orientation. Finally, the load was recovered by using the equation.

$$[F\ (t)] = \left[A_{optimum} * A_{optimum}\right]^{-1} * \left[A_{optimum}\right]^{T} * [\varepsilon\ (t)]_{optimum} \qquad (3.4)$$

3.2 Example of Static load Recovery

3.2.1 Flat Plate with a hole

Two numerical examples are presented next dealing with recovery of loads acting on a component. The first problem deals with recovery of two static loads acting on a flat plate with a central hole. The plate was modeled in ANSYS APDL. To reduce problem size, only quarter of the plate was modeled with a length of 100 units and width of 50 units. A circular hole of radius 10 units was created. Young's Modulus of 2e4 and Poisson's ratio of 0.3 were used as material properties. The meshing was done which resulted in 1218 elements. A unit load in X and Y directions was applied in two different steps and the strain data at all elements was extracted for both loading situations.

After the extraction of strain data form ANSYS, it was processed in MATLAB. The D-optimal design algorithm was implemented in MATLAB to find the optimum location and orientation of strain gages. As explained before, first the strains were transformed in all 18 directions by using Mohr's transformation and were subsequently processed by D-optimal design algorithm to find the optimum location and orientation angle. Four strain gages were mounted on optimal locations as shown in Figure 3.3.

In a separate simulation, the plate with the hole was subjected to load in both X and Y directions. The strains were extracted from ANSYS APDL corresponding to the optimum gage locations. Using the pseudo-inverse equation (Eq 3.4), the imposed load was estimated. The applied and recovered load were found to be in close agreement thereby validating inverse approach to load recovery.

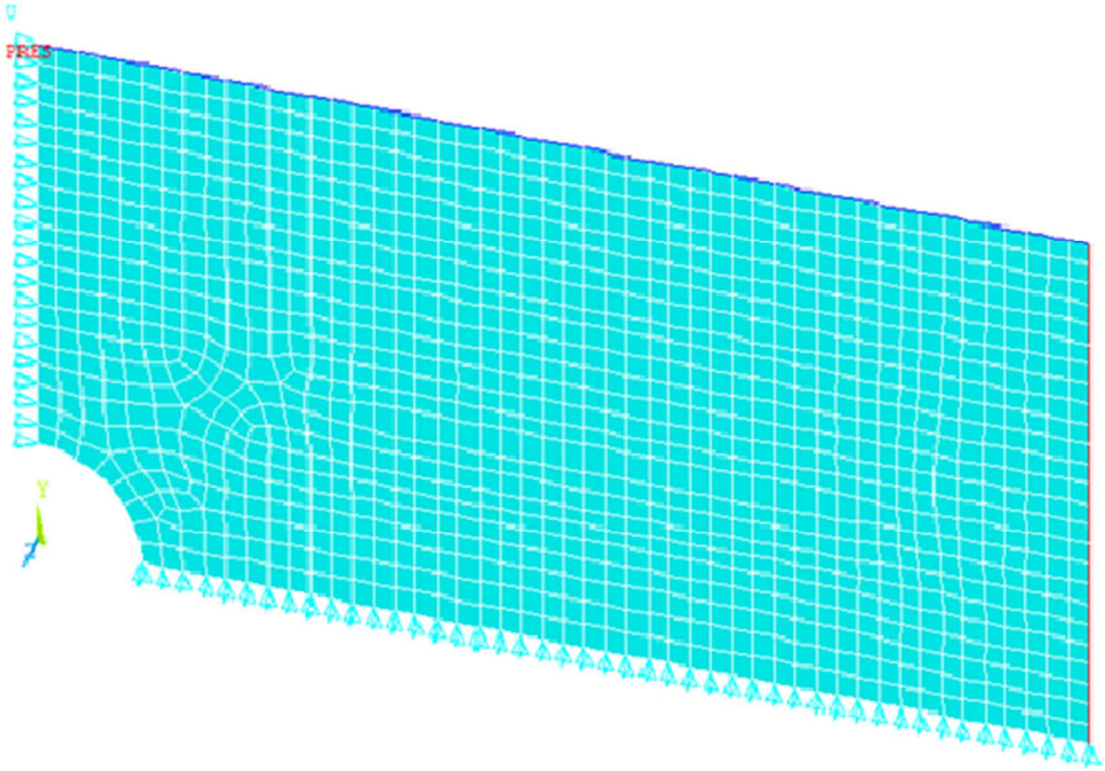

Figure 3.2: Flat Plate with a hole

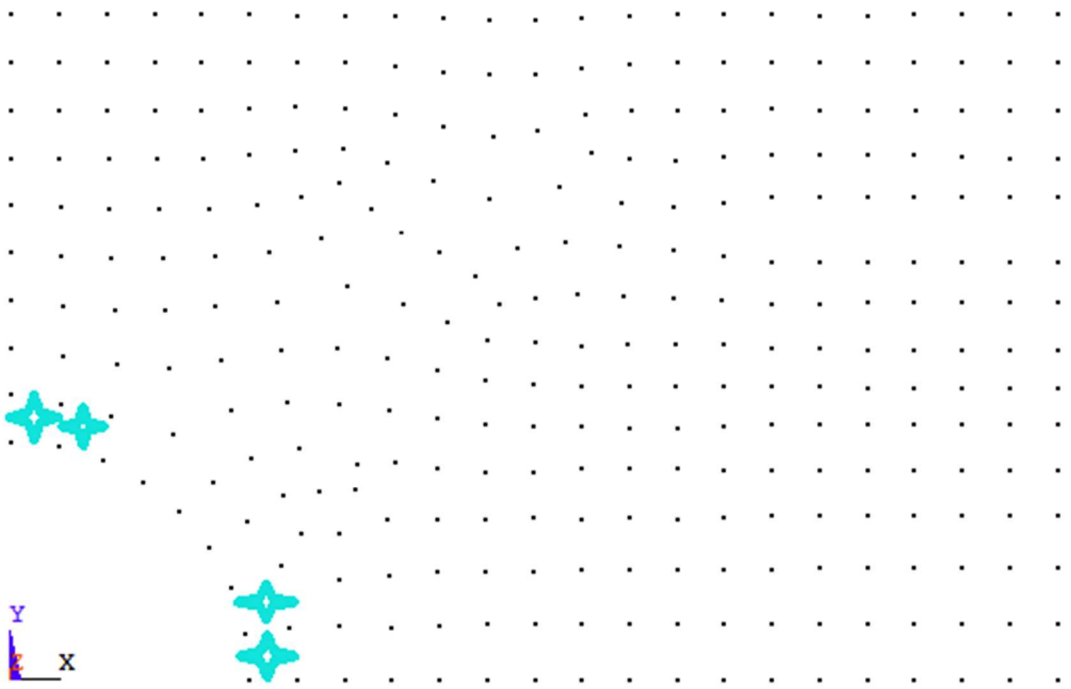

Figure 3.3 : Quarter Section of Plate with optimum gage locations

Table 3.1 : Optimum gage locations and Orientations angle

Optimum gage location	Orientation angle
1215	10
1216	170
1217	90
1218	0

Table 3.2: Results showing Applied loads and Recovered loads

Load direction	Applied load	Recovered load
X	20 N	19.99
Y	-50 N	-50.00

3.3 Quasi static Load Recovery

After load recovery in the static case, the algorithm was applied on a quasi-static case to further validate the D-optimal design algorithm. Quasi static loading is defined as the loading where inertial effects are negligible. In another words, the inertial forces are insignificant. To establish the fact that load recovery algorithm explained before works for quasi-static situations, a time varying loading is applied to a 3D cantilever beam in all three coordinate directions. The applied and recovered loads are compared for the entire duration of the application of three loads.

3.3.1 3D Cantilever beam

After the experiment on a plate with a hole, a slightly complicated model (3D cantilever beam) was subjected to three time varying loads. Solid92 elements were used in ANSYS to model a bent beam. The Young's modulus and Poisson's ratio were assumed to be 7.1e10 and 0.33 respectively. Meshing was done over the whole beam which resulted in 640 elements. Unit loads were applied in all three directions (X, Y and Z) at node number 579 (see Fig 3.4) in 3 different steps and elemental strain for all 640 elements was extracted for all 3 load cases. As before, all elemental strains were transformed in all 18 directions from 0 to 170 degrees in 10 degree increments. All the elemental strains along with all possible angular orientation were processed by D-optimal design algorithm to find the optimum location and orientation of strain gages.

The next step was to recover an applied load and compare it with the applied loads. In a separate simulation, three loads in all three directions were applied simultaneously and the elemental strains were extracted. Only the strain data corresponding to the optimum location and angular orientation were used on the pseudo inverse equation (Eq. 3.4) to recover the loads. As the results presented next will show the recovery was done and the recovered loads matched applied loads very well.

For this problem with three unknown loads, a total of five gages were used. The optimum gage locations and orientations are given in Table 3.2 and shown in Fig 3.5. The three applied loads consist of

(i) a sine load of amplitude of 1 unit applied in X-direction

(ii) a random load of magnitude ± 2 units applied in Y-direction

(iii) a square wave of amplitude 3 units applied in the Z-direction

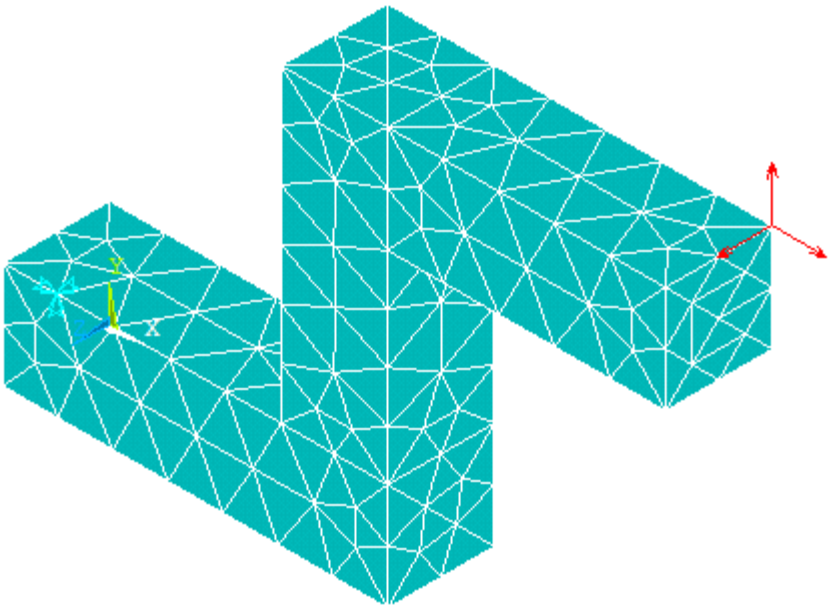

Figure 3.4: 3D bent beam with meshing, elements and force applied in X, Y and Z direction

Table 3.3: Optimum Gage locations and Orientations

Optimum Gage Location	Orientation angle
229	10
248	10
439	0
442	10
556	0

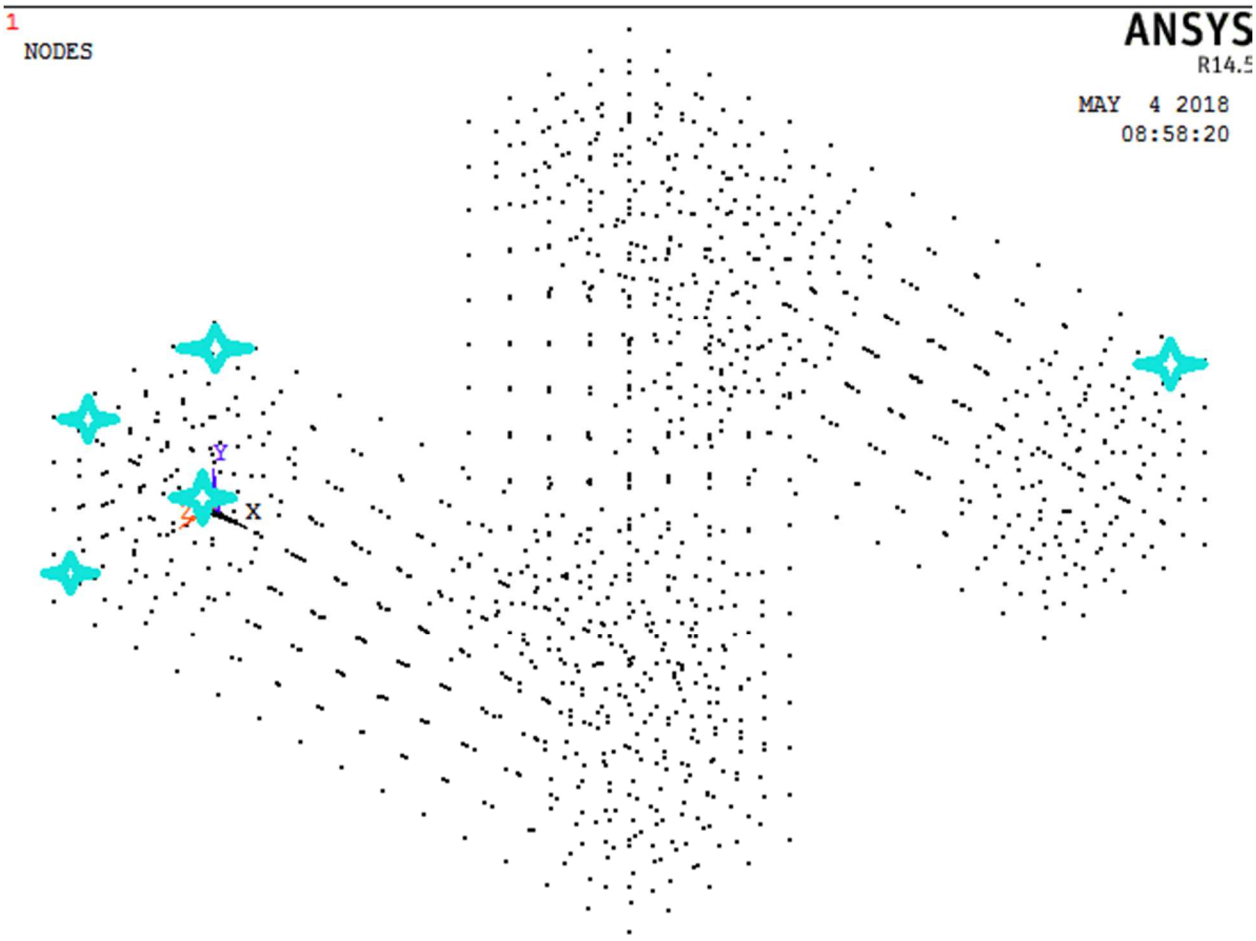

Figure 3.5: 3D cantilever beam showing optimum gage locations

3.3.2 Sinusoidal loading in X direction

For this case, the 3D cantilever beam is subjected to sinusoidal loading with the magnitude of 1 units applied from 0 to 1 second with a time step increment of 1/150 second. The loading was applied 150 times and all the elemental strain at all 150-time steps were extracted from ANSYS. Analysis of that data in MATLAB (D-optimal design algorithm, load recovery) resulted the recovery of applied load as shown in Figure 3.6. It can be seen that the applied load is recovered with a high degree of accuracy.

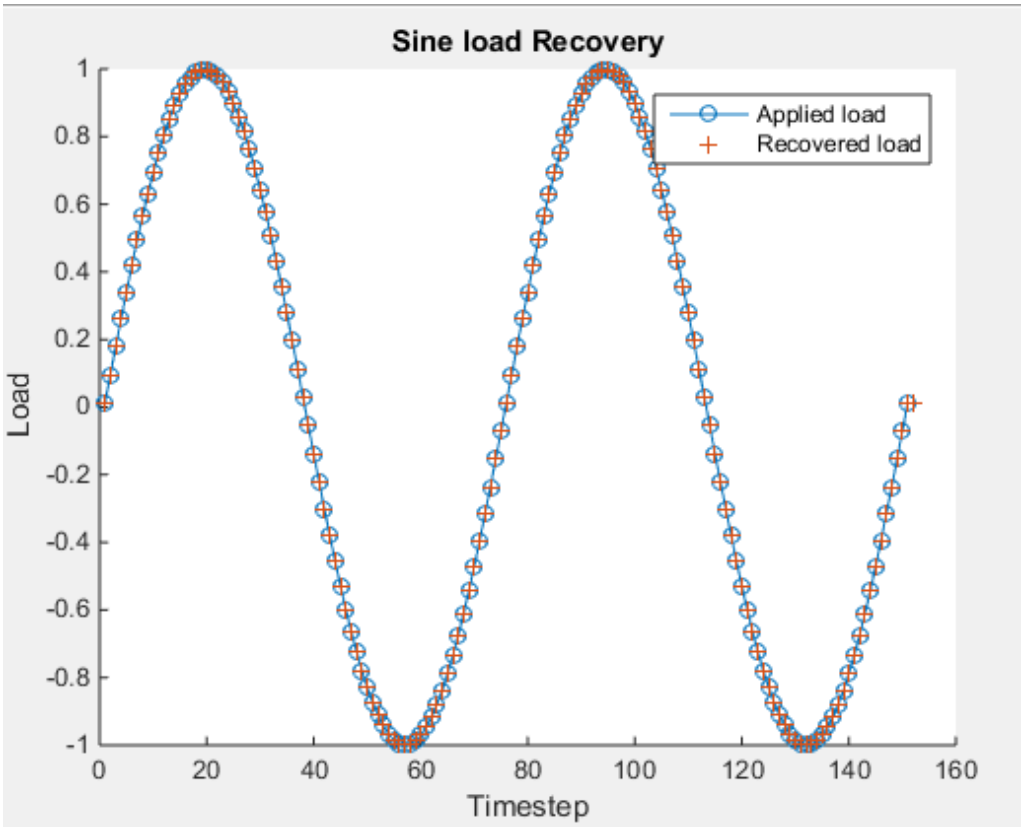

Figure 3.6 : Recovery of Sinusoidal load in X-direction

3.3.3 Random loading in Y direction

Random loading of magnitude between -2 units and +2 units was applied in the Y direction at node number 579 from 0 to 1 seconds. As before the loading was applied for 150 times and all the elemental strains at all 150-time steps were extracted. Analysis of data in MATLAB resulted the recovery of applied load as shown in figure 3.7. It can be seen that the applied random load is recovered with high degree of accuracy.

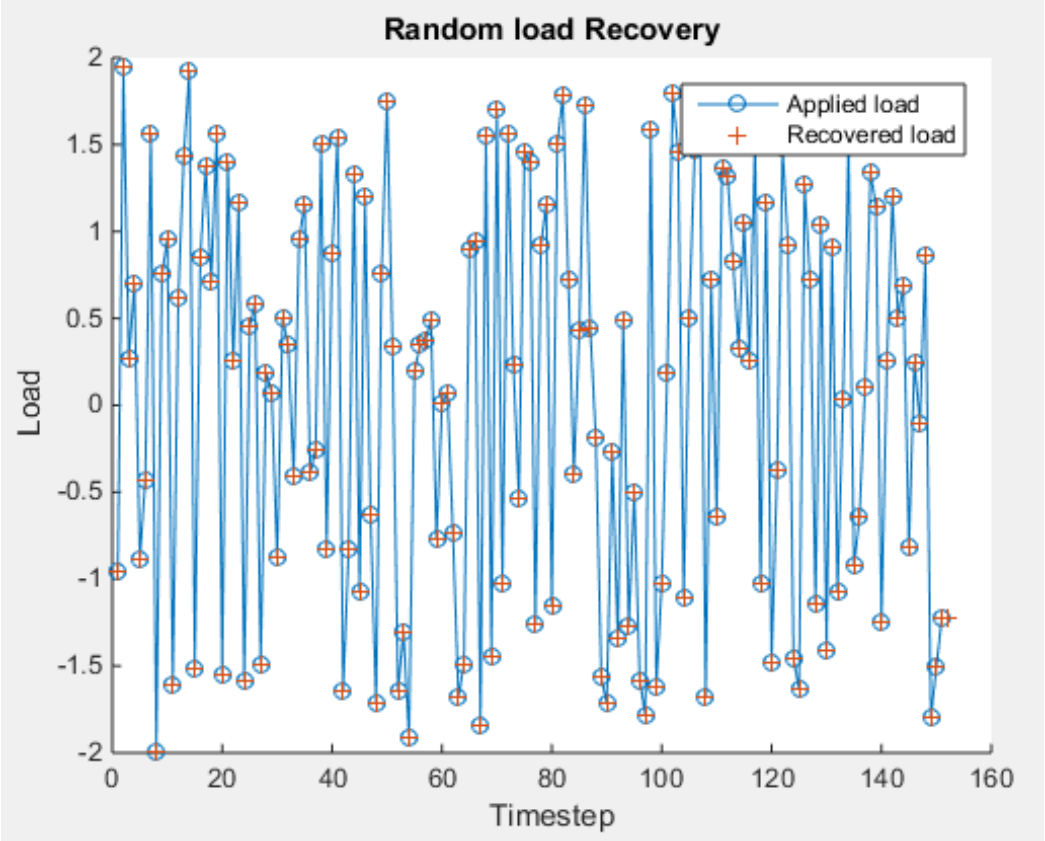

Figure 3.7: Recovery of Random load in Y-direction

3.3.4 Square loading in Z direction

For the final experiment in quasi-static loading, a square load of magnitude 3 units was applied in the node number 579 and the elemental strains were extracted. Analysis of those data in MATLAB (D-optimal design algorithm, load recovery) resulted in the recovery of applied load as shown in Fig 3.8. As expected, it can be seen that the applied load is recovered with a high degree of accuracy.

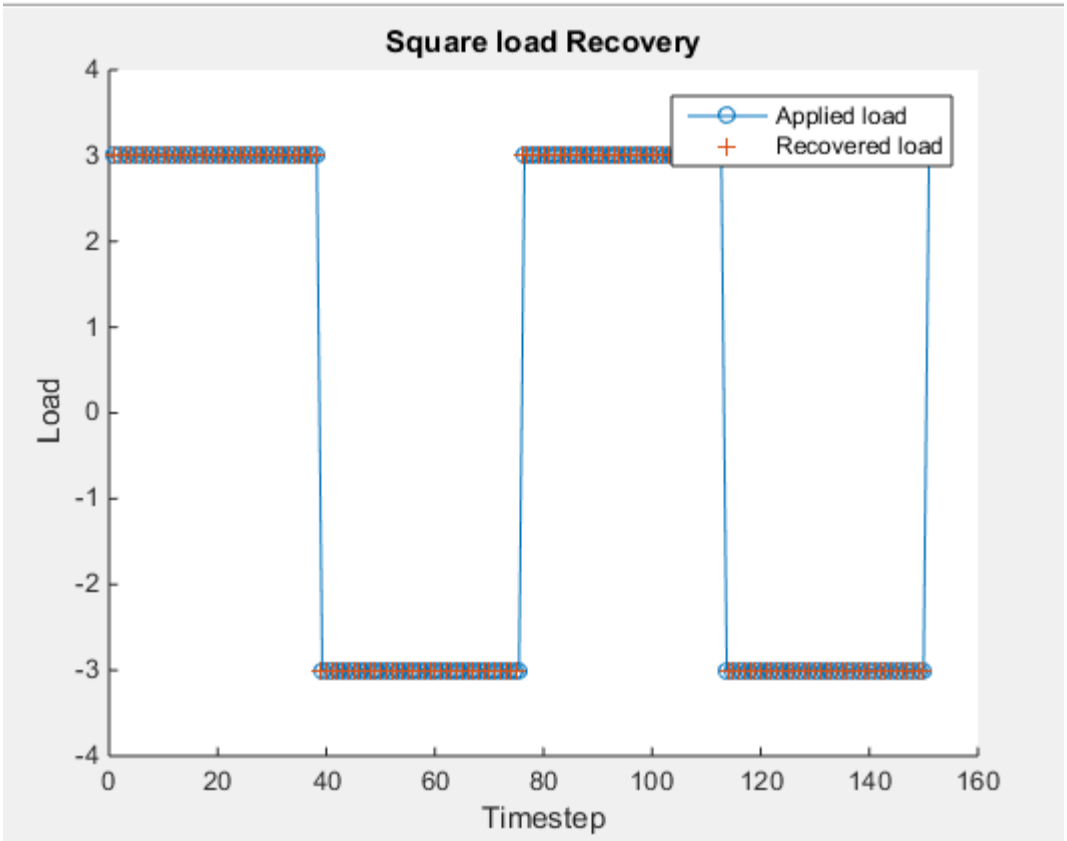

Figure 3.8: Recovery of square wave load in Z- direction

3.4 Summary

This chapter presented an application of D-optimal design algorithm on two problems dealing with the recovery of static and quasi-static loads. For the static case, a flat plate with a hole was used as an example of 2D static load recovery. A 2D plate with a hole was modeled in ANSYS APDL, the strains values were extracted and D-optimal design algorithm was used to find the optimum gage locations. Finally, the recovery of an unknown load was done by using strain data obtained from optimum locations. It is seen that applied loads are recovered with high accuracy.

Next, a 3D bent cantilever beam was modeled in ANSYS APDL and three time varying loads were applied simultaneously. Once again, all three loads were recovered with a high degree of accuracy thereby confirming the effectiveness of the proposed approach.

4 Transient Load Recovery using Strain measurements and Model Reduction

The recovery of transient loads using strain measurements is discussed in this chapter. Using a cantilever beam as a test example which is subjected to transient loading conditions, nodal displacements and accelerations are recovered using mode participation factor and mode shapes. Furthermore, Craig- Bampton reduction technique is used to reduce the problem size without adversely affecting the quality of recovered loads.

4.1 Theoretical Development

For the purpose of this chapter, transient loading is defined as the loading condition where imposed loads are time dependent and inertial effect are present. It differs from the quasi-static loading considered in the previous chapter in that in case of transient loading, the inertial effects are present whereas inertial effects were not considered in case of quasi-static loading. The process of recovery of transient loads is explained in detail in this chapter.

4.1.1 Modal Analysis and Extraction of Strain Modes

The first step in the recovery of transient loads is to perform a modal analysis of the structure and to extract the normal displacement modes as well as strain modes. The component in question is modeled in ANSYS, modal analysis of the system is performed in ANSYS APDL and mode shapes for all the modes are extracted. Each mode shape is applied as displacement input at all nodes to extract the strain mode of the component. Both the displacement mode shapes and strain mode shapes are intrinsic dynamic characteristics of the system and both of them could be used for research. However, for sensitivity reasons, strain modes will be used in this research. The strain modes are used to calculate the mode participation factor.

The relationship between strain modes, strains and mode participation factor is given by,

$$\{\varepsilon(t)\} = [\Psi^{\varepsilon}]\{q(t)\} \quad (4.1)$$

where, $\varepsilon(t)$ is strain, $[\Psi^{\varepsilon}]$ is strain mode and $\{q(t)\}$ is mode participation factor.

However, in real world problems, strain modes for all degree of freedom are hardly available but strain modes for finite number of modes could be obtained from finite element analysis. So, equation 4.1 can be reduced to,

$$\{\varepsilon(t)\} = [\Psi_m^{\varepsilon}]\{q_m(t)\} \quad (4.2)$$

.

where, $\{q_m(t)\}$ and $[\Psi_m^{\varepsilon}]$ are mode participation factor and mode shapes for retained modes respectively. Equation 4.2 could be modified to solve for $\{q_m(t)\}$ as follows,

$$\{q_m(t)\} = ([\Psi_m^{\varepsilon}]^t[\Psi_m^{\varepsilon}])^{-1}[\Psi_m^{\varepsilon}]^t\{\varepsilon(t)\} \quad (4.3)$$

So, from the above equation, if the strain values and strain modes are known, mode participation factor could be calculated.

4.1.2 Strain Extraction at optimum locations

Equation 4.3 describes the way to effectively calculate the mode participation factor using strain values. However, it requires strain data from all locations on the component. Since it is impossible to extract strain values at all surface locations, strain should be extracted at specific optimum locations. Section 3.1.2 explicitly explained the algorithm used to select the optimum locations. First a candidate set is chosen where the strain gages could be possibly mounted. The D-optimal design algorithm discussed in chapter 3 can be used on the candidate set to get the

optimum locations where the strain gages are mounted and the strain data at these optimum location is extracted. So, equation 4.3 could be rewritten as,

$$\{q_m(t)\} \cong \{q_m(t)\}_{opt} = ([\Psi_m^{\varepsilon}]_{opt}^t[\Psi_m^{\varepsilon}]_{opt})^{-1}[\Psi_m^{\varepsilon}]_{opt}^t\{\varepsilon(t)\}_{opt} \quad (4.4)$$

4.1.3 Displacement, Velocity and Acceleration Computation and Force Recovery

After the computation of mode participation factor, displacement, velocity and acceleration can be computed for any node by using standard formulas given below:

$$\{x(t)\} = [\Phi]\{q(t)\} \quad (4.5)$$

$$\{\dot{x}(t)\} = [\Phi]\{\dot{q}(t)\} \quad (4.6)$$

$$\{\ddot{x}(t)\} = [\Phi]\{\ddot{q}(t)\} \quad (4.7)$$

Here $\{x(t)\}$ is displacement, $[\Phi]$ is the matrix containing displacement mode shapes and $\{q(t)\}$ is mode participation factor. After computation of $\{x(t)\}$, $\{\dot{x}(t)\}$ and $\{\ddot{x}(t)\}$, load could be recovered by using the equation,

$$[M]\ddot{x}(t) + [C]\dot{x}(t) + [K]x(t) = F(t) \quad (4.8)$$

Here [M], [C] and [K] are mass, damping and stiffness matrix respectively and could be obtained from ANSYS APDL in Harwell Boeing Format. The applied load could be recovered using equation (4.8) above, however, this method requires mode participation factor to be recovered for all modes which is often impractical. The number of retained modes is governed by number of strain gages used which is also governed by cost considerations. So, exact load recovery using this procedure is not feasible. A more feasible method is introduced below which utilizes model reduction.

4.1.4 Load Recovery from Model Order Reduction

Load Recovery by retaining all strain or normal modes is impractical and expensive. So, an alternative method is required to recover the load using a subset of strain or normal modes. One alternative method is Model Order Reduction. Model Order Reduction reduces the large stiffness, mass and damping matrices to smaller sized matrices such that the model properties are captured as completely as possible. Static Condensation (Guyan Reduction) and Craig-Bampton Reduction are two such methods that are implemented in this research. Both of them are described briefly next.

4.1.4.1 Guyan Reduction (Static Condensation)

Guyan Reduction, also called Static Condensation, is commonly used reduction technique. It reduces the number of degrees of freedom by ignoring the inertial terms of the equilibrium equation and the expressing the unloaded degrees of freedom in terms of loaded degrees of freedom. The loaded degrees of freedom and unloaded degrees of freedom are also called master degree of freedom and slave degree of freedom respectively.

After partitioning the nodal degrees of freedom into master (x_m) and slave (x_s) degrees of freedom and ignoring the inertial terms and damping terms, Eq. (4.8) can be written as

$$\begin{bmatrix} K_{mm} & K_{ms} \\ K_{ms} & K_{ss} \end{bmatrix} \begin{pmatrix} x_m(t) \\ x_s(t) \end{pmatrix} = \begin{pmatrix} F_m(t) \\ F_s(t) \end{pmatrix} \quad (4.9)$$

where, K refers to the stiffness matrix, x (t) refers to the displacement and F (t) refers to the force, subscript 'm' refers to master degrees of freedom and 's' refers to the slave degree of freedom. The degrees of freedom where the load is not applied are considered as slave degrees of freedom, so, F_s (t) is equal to zero. Thus, the second part of the equation (4.9) reduces to

$$[K_{sm}]\{x_m(t)\} + [K_{ss}]\{x_s(t) = F_s(t) = 0 \quad (4.10)$$

The slave degrees of freedom can be written as in terms of master degrees of freedom displacements as,

$$\{x_s(t)\} = -[K_{ss}]^{-1}[K_{ms}]\{x_m(t)\} \quad (4.11)$$

The combination of slave and master degrees of freedom can be expressed as,

$$\{x(t)\} = \begin{Bmatrix} x_m(t) \\ x_s(t) \end{Bmatrix} = \begin{bmatrix} I \\ -K_{ss}^{-1}K_{ms} \end{bmatrix} \{x_m(t)\} \quad (4.12)$$

where I is identity matrix, and $\begin{bmatrix} I \\ -K_{ss}^{-1}K_{ms} \end{bmatrix}$ is called Guyan Transformation matrix (T_{guyan}). The transformation matrix (T_{guyan}) could be used to reduce the mass, stiffness and forcing matrices of the full model by using the equation below,

$$[M_{guyan}] = [T_{guyan}^T][M][T_{guyan}] \quad (4.13)$$

$$[K_{guyan}] = [T_{guyan}^T][K][T_{guyan}] \tag{4.14}$$

$$[F_{guyan}] = [T_{guyan}^T][F] \tag{4.15}$$

4.1.4.2 Craig Bampton Reduction

Craig Bampton Reduction, also called Component Mode Synthesis, is widely used method to reduce large dynamic models. It is better than the Guyan reduction in way that it retains inertial effects and hence is more accurate than Guyan reduction. Similar to the Guyan reduction, the total degree of freedom are divided into boundary degrees of freedom and internal degrees of freedom. The degrees of freedom where forces are applied are retained as boundary degrees of freedom and most of the degrees of freedom where force is not applied are considered as internal degrees of freedom. However, some degrees of freedom where forces are not applied could also be considered as boundary degrees of freedom. These degrees of freedom are shared across multiple substructure. The equation of system, ignoring damping, are given by,

$$\begin{bmatrix} M_{bb} & M_{bi} \\ M_{bi} & M_{ii} \end{bmatrix} \begin{Bmatrix} \ddot{x_b}(t) \\ \ddot{x_i}(t) \end{Bmatrix} + \begin{bmatrix} K_{bb} & K_{bi} \\ K_{bi} & K_{ii} \end{bmatrix} \begin{Bmatrix} x_b(t) \\ x_i(t) \end{Bmatrix} = \begin{Bmatrix} F_b(t) \\ F_i(t) \end{Bmatrix} \tag{4.16}$$

To capture the inertial effects, both normal modes and static modes are used.

a) Normal Mode of structure

Craig-Bampton reduction method uses the inertial terms to improve the accuracy of reduction. To capture the inertial terms, normal modes of the structure are computed by solving the eigenvalue problem given in Eqn. (4.17)

$$-\omega^2[M_{ii}] + [K_{ii}] = \{0\} \tag{4.17}$$

Solution to the above eigenvalue problem gives constrained modal matrix $[\Phi]_c$, and constrained normal modes $\{x(t)\}_i^n$ given by

$$\{x(t)\}_i^n = [\Phi]_c\{q(t)\}_p \tag{4.18}$$

where p is the number of Craig-Bampton constraint modes

b) Static modes of structure

The static modes of a structure in CB reduction are computed in similar way as was done in Guyan reduction. This is shown in equation below.

$$\{x(t)\}_i^s = -[K]_{ii}^{-1} * [K]_{ib}\{x(t)\}_b \tag{4.19}$$

The full displacement vector {x (t)} is now given by,

$$\{x(t)\} = \begin{Bmatrix} x(t)_b \\ x(t)_i \end{Bmatrix} = \begin{Bmatrix} \{x(t)_b \\ -[K]_{ii}^{-1}[K]_{ib}\{x(t)\}_b + [\Phi]_c\{q(t)\}_p \end{Bmatrix} \tag{4.20}$$

The equation above could be further simplified as

$$\{x(t)\} = [T_{cb}]\begin{Bmatrix} x(t)_b \\ x(t)_i \end{Bmatrix} \tag{4.21}$$

where,

$$[T_{cb}] = \begin{bmatrix} [I] & [0] \\ -[K]_{ii}^{-1}[K]_{ib}\{x(t)\}_b & [\Phi]_c \end{bmatrix} \tag{4.22}$$

The reduced mass, stiffness and damping matrices is given by the following equations respectively:

$$[M]_{CB} = [T_{cb}]^T [M][T_{cb}] \tag{4.23}$$

$$[K]_{cb} = [T_{cb}]^T [K][T_{cb}] \tag{4.24}$$

$$[C]_{cb} = [T_{cb}]^T [C][T_{cb}] \tag{4.25}$$

Finally, the applied force is recovered by using the equation:

$$[M]_{CB}\ddot{x}(t)_b + [C]_{CB}\dot{x}\,(t)_b + [\,K]_{CB}x(t)_b = F(t)_b \tag{4.26}$$

4.2 Examples of Load Recovery

A 3D cantilever beam made of aluminum was modeled in ANSYS APDL. SOLID45 elements were used to create the model. Young's Modulus value of 71e9 and Poisson's ratio of 0.33 was used for the example. The length, width and thickness of the beam used in the model were 0.25 m, 0.05 m and 0.003m. All the properties of aluminum were input and mapped meshing was done to create 200 elements with 600 degrees of freedom. The mass matrix [M] and stiffness matrix [K] were extracted in Harwell-Boeing format and were converted to standard form in MATLAB. A sinusoidal forcing function F_y= 8000sin (30t) was applied at node 149 in the Y-direction as shown in Fig. 4.1 below.

A total of seven modes were extracted for this beam using ANSYS. Since seven modes will be used in the analysis, the number of gages needed must be greater than or equal to 7. A

total of eight strain gages are used in this example. Using the D-optimal design algorithm presented in Chapter 3, the optimum locations and orientation of the eight gages are given in Table 4.1 with gage placement on the beam shown in Fig. 4.2.

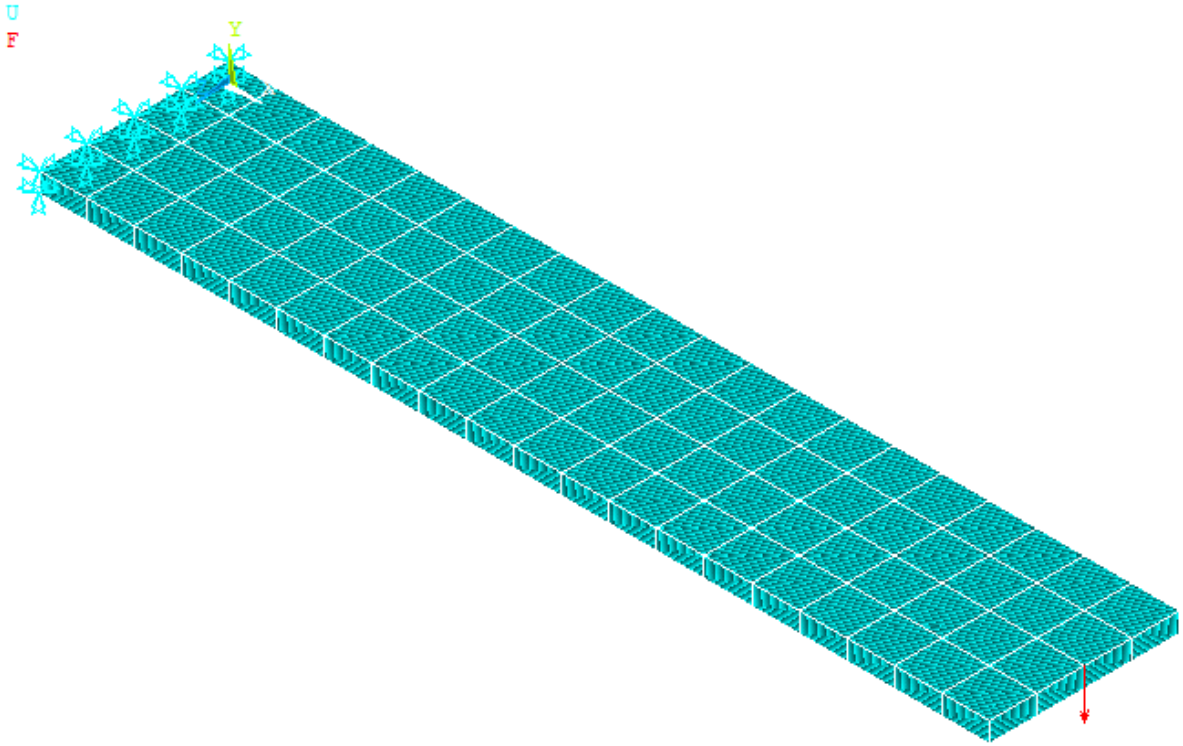

Figure 4.1 :3D cantilever beam showing applied force in Y direction at node 149

Table 4.1: Optimum gage locations and orientation angles

Optimum gage location	Orientation Angle
86	90
208	40
176	100
240	90
237	70
231	100
180	90
160	90

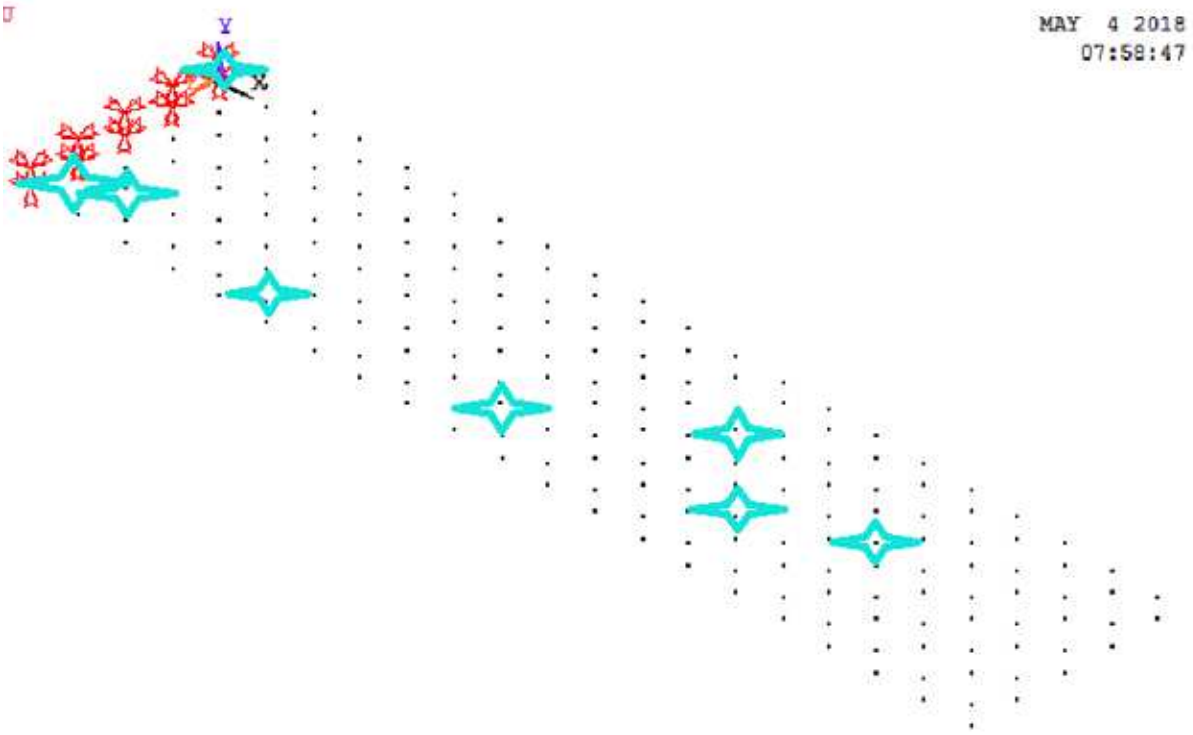

Figure 4.2: 3D cantilever beam showing optimum gage locations

The strain modes shapes, displacement modes shapes and mode participation factor for 17 modes were extracted using ANSYS APDL. It was seen that only 7 of 17 modes could be used as they corresponded to transverse mode of vibration. Using the seven modes, a total of 8 gauges were placed on the structure and strains at optimum location was extracted. Equation 4.4 was used to calculate the mode participation factor of the seven modes. After MPF were recovered, displacement and acceleration were calculated using equation 4.5 and equation 4.7. Next, the applied force was reconstructed with equation 4.8. It can be seen from Fig. 4.3-4.5, that the mode participation factors are recovered accurately. The MPF value extracted from ANSYS and those calculated using Eq.(4.4) match well. However, as figure 4.6 shows, when Eq. (4.8) is used to estimate applied load, the results are poor.

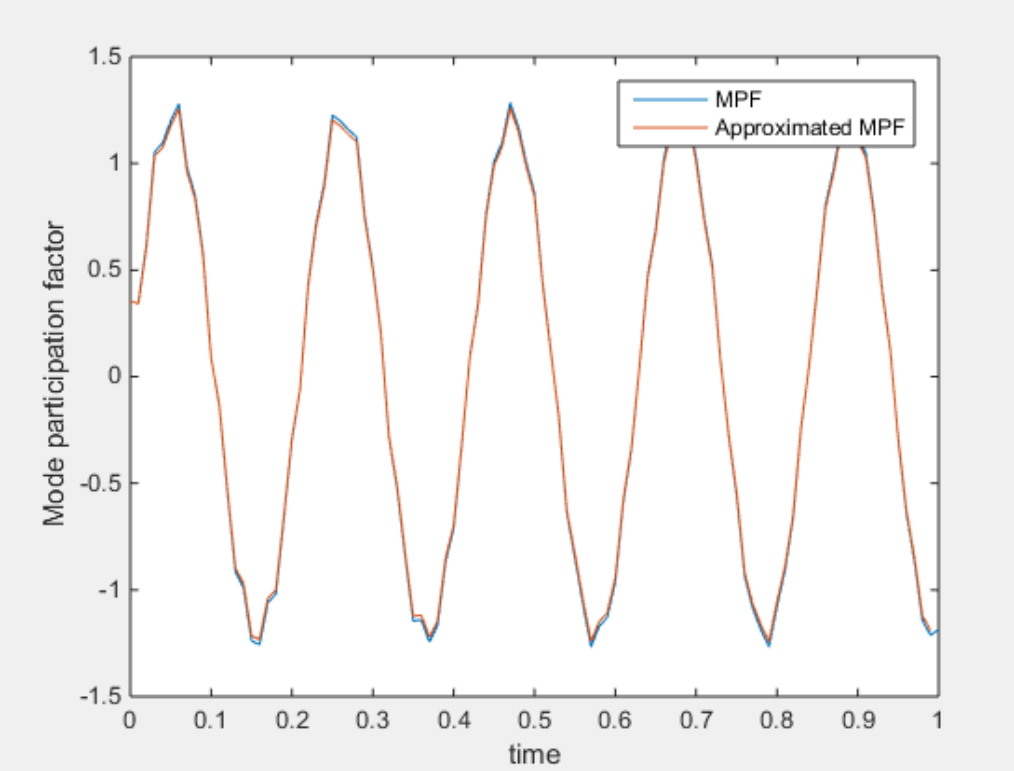

Figure 4.3 : Mode participation factor for mode 1

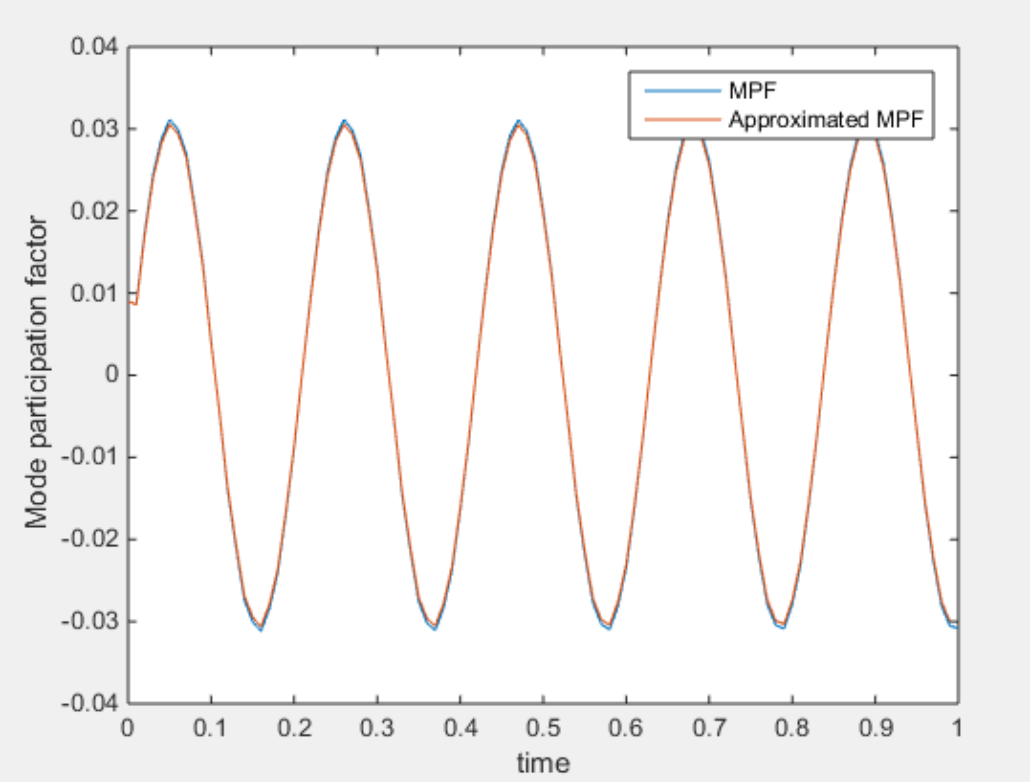

Figure 4.4 : Mode participation factor for mode 2

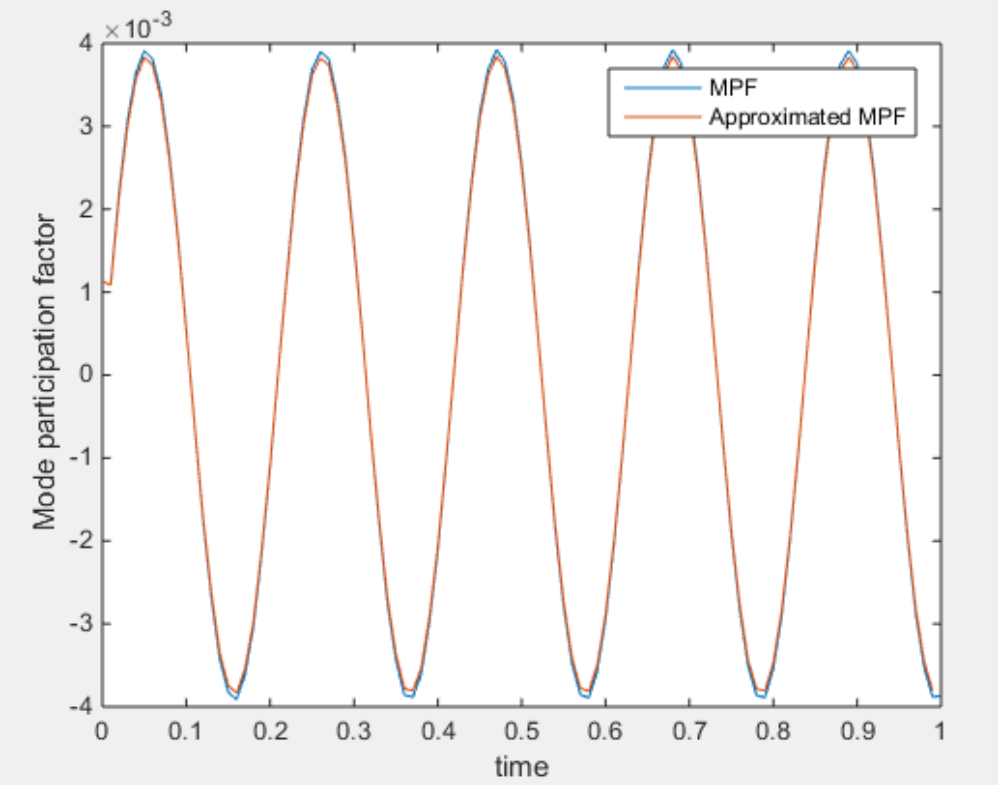

Figure 4.5 : Mode participation factor for mode 5

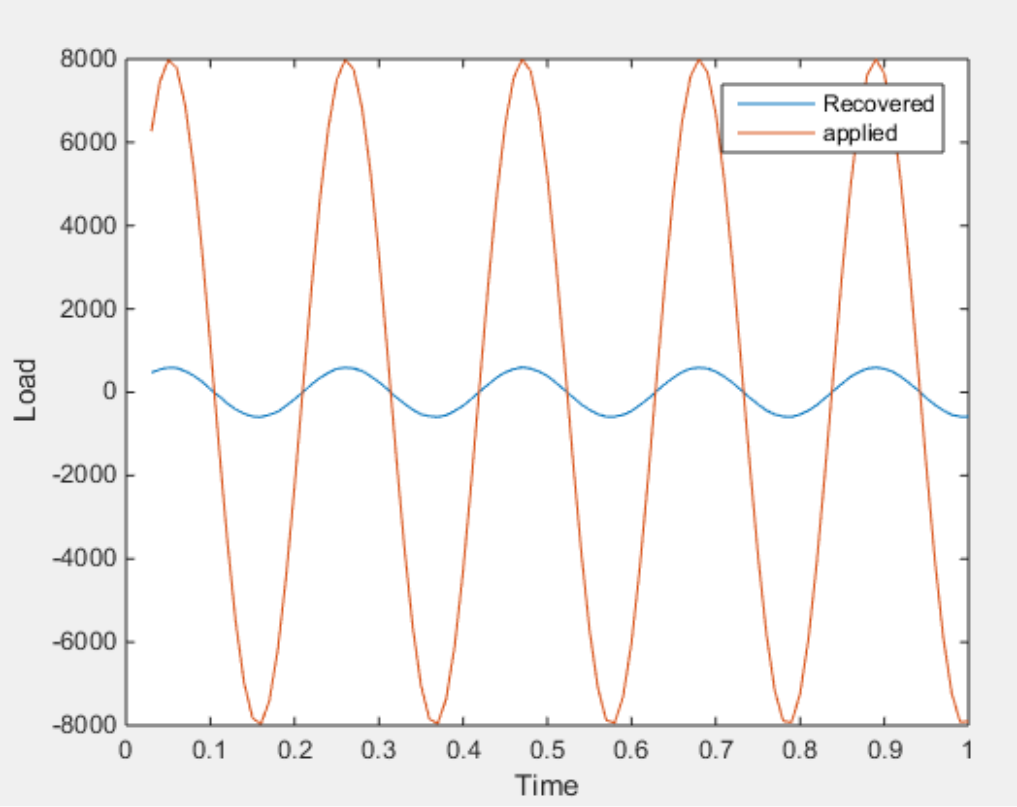

Figure 4.6 : Applied load and recovered load with 7 retained modes

To fix this problem, model order reduction based on CB reduction was used to improve load estimates. Using seven normal modes, eight gages and four boundary degrees of freedom and Eq. (4.26), the applied load was estimated. As seen in Figure 4.7, CB reduction results in significant improvement in load estimation.

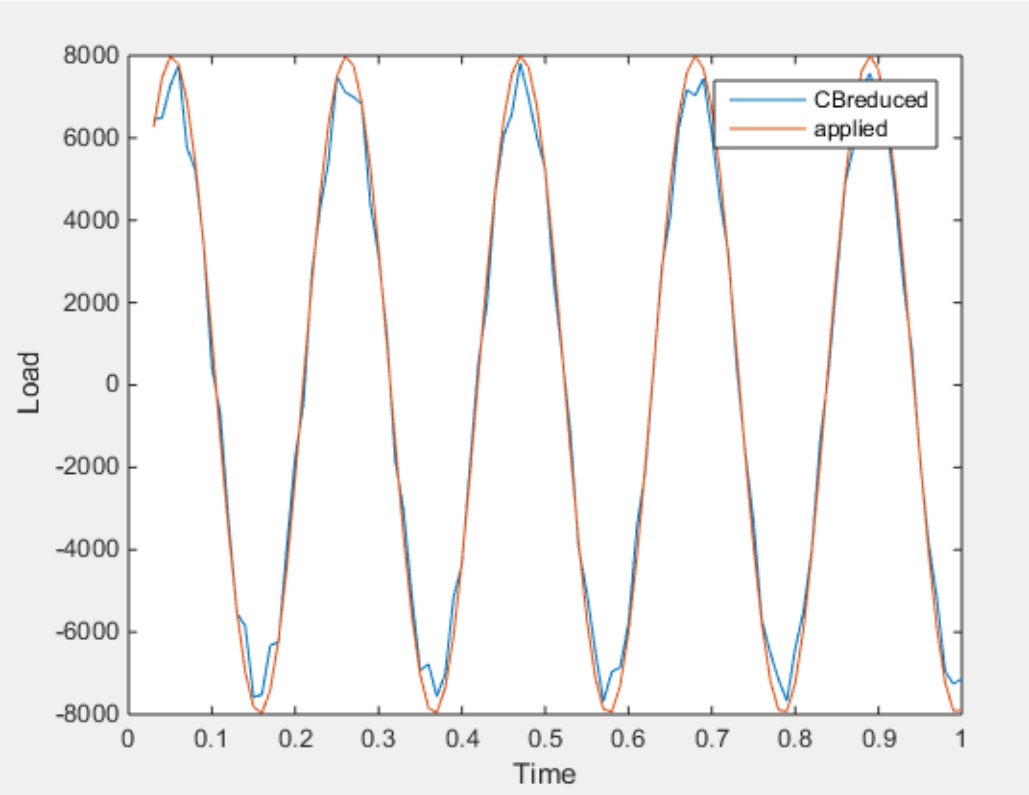

4.2.1 Load Recovery Based on Response Simulation using ODE 45

Instead of using the data from ANSYS APDL to recover the applied loads, MATLAB built-in function ODE45 was also used to simulate the system response to applied loading. Since the complete stiffness matrix and mass matrix are of size 600 by 600, using the full model to simulate the system response is extremely time consuming and expensive. Therefore, the full model was reduced to a 6 by 6 system by using CB reduction and the reduced order CB model

was used to recover the displacement and acceleration data. By using the equation below, the applied load was recovered,

$$[M]_{CB}\ddot{x}(t)_b + [C]_{CB}\dot{x}\,(t)_b + [K]_{CB}x(t)_b = F(t)_b \qquad (4.27)$$

Here $[M]_{CB}$, $[C]_{CB}$, $[K]_{CB}$ are Craig-Bampton reduced mass, damping and stiffness matrices respectively.

Figure 4.9 shows the graph of displacement data at node 149 approximated using ANSYS results as well as those obtained from ODE45 simulation. Both approaches utilize CB reduction. A close agreement between ANSYS and ODE45 results indicates that 6 by 6 reduced order model is able to capture the dynamics of the complete 600 by 600 model with a reasonable accuracy.

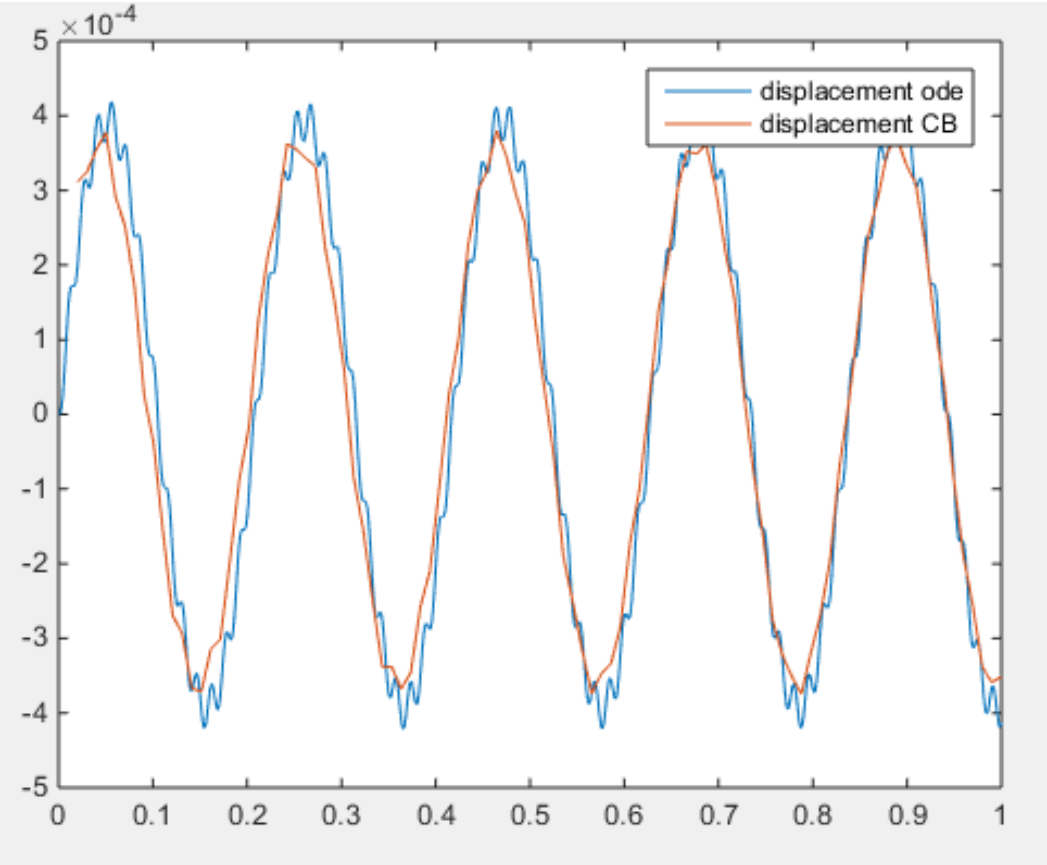

Figure 4.7: Displacement of node 149 using ANSYS data and ODE45 simulation

4.3 Summary

In this chapter, load recovery is done on a 3D cantilever beam using strain data from measurements. The recovery is done with as well as without model order reduction. It is seen that without using reduction, it is hard to recover applied load because MPF for all modes need to be considered which requires strain gages to be placed at all locations. This is quite impractical. However, with CB reduction, the load was recovered accurately by retaining only 7 out of 600 modes. The results illustrate that modal order reduction techniques show considerable promise in helping obtain reasonably accurate load estimates while using only a small subset of modal information.

5 Impact Load Recovery using Strain Measurements and Model Order Reduction

Impact loads on structural components are of particular interest to engineers. Impact loading is naturally occurring phenomena in many structures and can lead to disastrous consequences. The breakup of space shuttle Colombia is one such example. Such a catastrophic outcome has motivated extensive research in this field. In this chapter, impact loads acting on a component will be estimated. Impact loads are applied on an aluminum plate and loads are recovered using strain measurement at optimum gage locations on the component and by using model order reduction. The displacement mode shapes and strain mode shapes of the component will be extracted from ANSYS APDL. The strain mode shapes and strain data will be used to calculate mode participation factor. The approximated mode participation factor and displacement mode shapes will be used to approximate displacement, velocity and acceleration at all nodes of the structure under consideration. The approximated displacement, velocity and acceleration data will be used to estimate the imposed load on the structure.

5.1 Theoretical Development

As described in the previous chapter, impact load will be recovered by measuring strain data at optimum strain gage locations. Displacement and acceleration data will be approximated using displacement mode shapes and approximated mode participation factors. The impact load will be recovered without using model order reduction as well as reduction techniques. Reduction techniques like Guyan Reduction and Craig-Bampton are used to recover the load. Both static and dynamic condensations methods are used to recover the load. Load recovery without reduction techniques is also possible but requires lot more strain gages to be mounted on

the structure and strain mode shapes and displacement modes of a large number of modes are required. Since, the placement of strain gages at all locations is impossible and information of strain and displacement mode shape at all modes is not possible, CB reduction technique is most effective technique to recover the load while employing limited modal information.

5.1.1 Load Recovery using simulated data from ANSYS APDL

As described in the previous chapter, the structure was modeled in ANSYS APDL and the loading was applied. The displacement mode shapes and strain mode shapes were extracted for 30 modes. The strain data at optimum locations was also extracted and strain data and strain modes shapes were used to approximate the mode participation factors. Displacement mode shapes and approximated mode participation factor were used to calculate displacement and acceleration. Equation 5.1 was finally used to recover the impact loading.

$$[M][\Phi]\{\ddot{q}(t)\} + [C][\Phi]\{\dot{q}(t)\} + [K][\Phi]\{q(t)\} = F(t) \qquad (5.1)$$

However, extracting strain data at all nodes is infeasible. So, model reduction (CB reduction and Guyan reduction) was done on the system. The advantages of the model reduction is that load could be successfully recovered using reduced matrix that requires information for fewer number of strain modes and displacement modes. The impact load is recovered using the following equation,

$$[M]_{CB}\ddot{x}(t)_b + [C]_{CB}\dot{x}(t)_b + [K]_{CB}x(t)_b = F(t)_b \qquad (5.2)$$

where, $[M]_{CB}$,$[C]_{CB}$, $[K]_{CB}$ are Craig Bampton reduced mass, damping and stiffness matrices. Similarly, load also could be recovered using Guyan Reduction.

$$[F_{guyan}] = [T_{guyan}^T][F] \qquad (5.3)$$

where, $[T_{guyan}^{T}]$ is Guyan transformation matrix as discussed previously in chapter 4.

5.1.2 Error Quantification

The quality of load estimation can be determined by examining the difference between the applied load and the recovered load. The error in the recovered load can be quantified by using the root mean square (rms) error. The percentage root mean square (rms) error $\boldsymbol{\varepsilon}_{\text{rms}}$ in recovered loads with respect to the actual applied load is calculated as,

$$\boldsymbol{\varepsilon}_{\%\mathbf{rms}} = \left(\frac{\sqrt{\sum (force_{applied} - force_{recovered})^2}}{\sqrt{\sum force_{applied}^2}} \right) * 100 \tag{5.4}$$

5.1.3 Material Damping

While dealing with impact loading, the load recovery process assumes that the internal material damping can be modelled as Rayleigh damping. The damping matrix is assumed to be a linear combination of mass and stiffness matrices. The equation for the damping coefficient is given by,

$$\xi = \frac{\alpha}{2\omega_i} + \frac{\beta \omega_i}{2} \tag{5.5}$$

where, α and β are damping coefficient and ω_i is natural frequency. By adjusting the value of α and β, the damping ratio can be set to a desired value. In this research, we have assumed a ξ value equal to 0.01 for the first vibration mode.

5.2 Example of Load Recovery on an aluminum plate

The recovery of impact loads will be demonstrated using an aluminum plate that is clamped along all four edges. The aluminum plate was modeled in ANSYS APDL. Solid element (SOLID45) was used to create the finite element model. The Young's modulus value of 71e9 and Poisson's ratio of 0.33 was used for the plate material. The length, width and thickness of the plate were 0.8 m, 0.6m and 0.008m respectively. All the properties of aluminum were input and mapped meshing was done to generate finite element mesh. The mass matrix [M] and stiffness matrix [K] were extracted in Harwell-Boeing format and was converted to standard form in MATLAB. All the four edges of the plate were fixed and impact loading was applied as shown in Figure 5.1 Triangular wave loading, square wave loading and half sine-wave impact loading were the three types of impact loads applied on the aluminum plate. The recovery of all three loads is briefly discussed below.

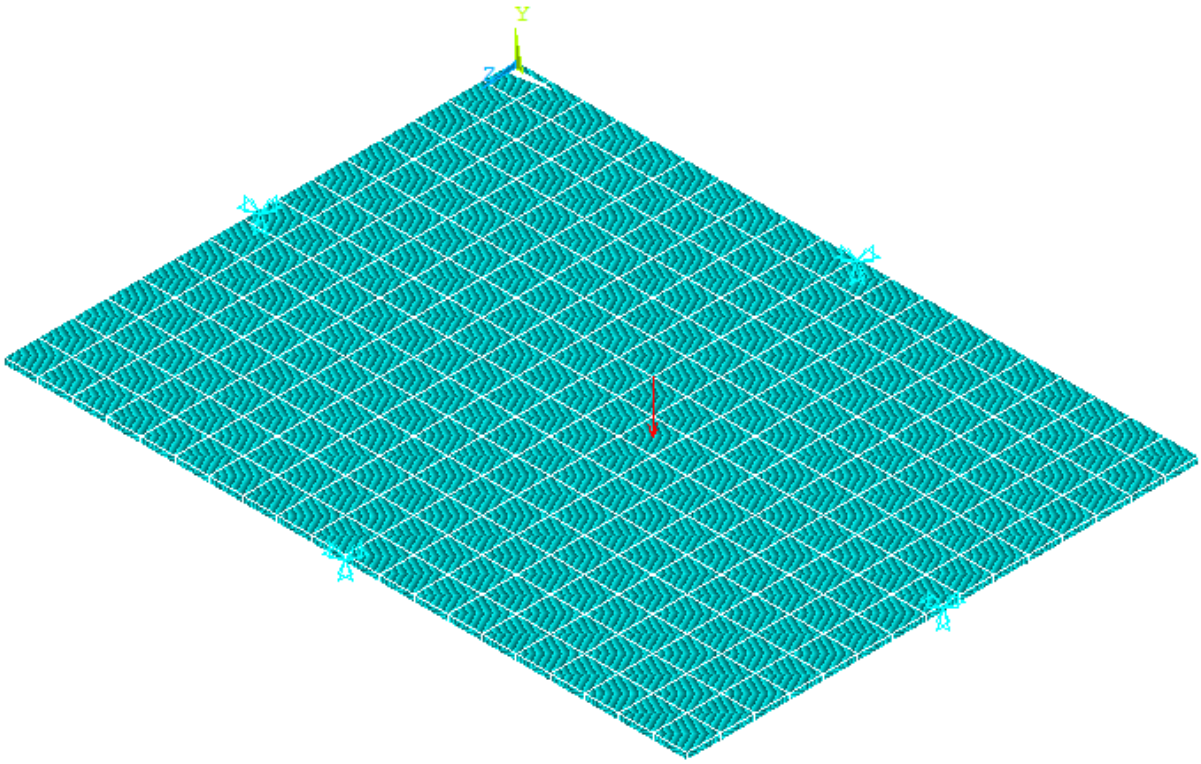

Figure 5.1: Flat plate constrained along four edges with impact load

A total of eight strain gages are located on the plate. The optimum gage locations and orientations are given in Table 5.1 and the corresponding positions on the plate are shown in Fig. 5.2.

Table 5.1: Optimum gage locations and orientation angles

Optimum gage location	Orientation angle
608	0
892	0
420	90
781	90
312	0
588	0
500	90
701	90

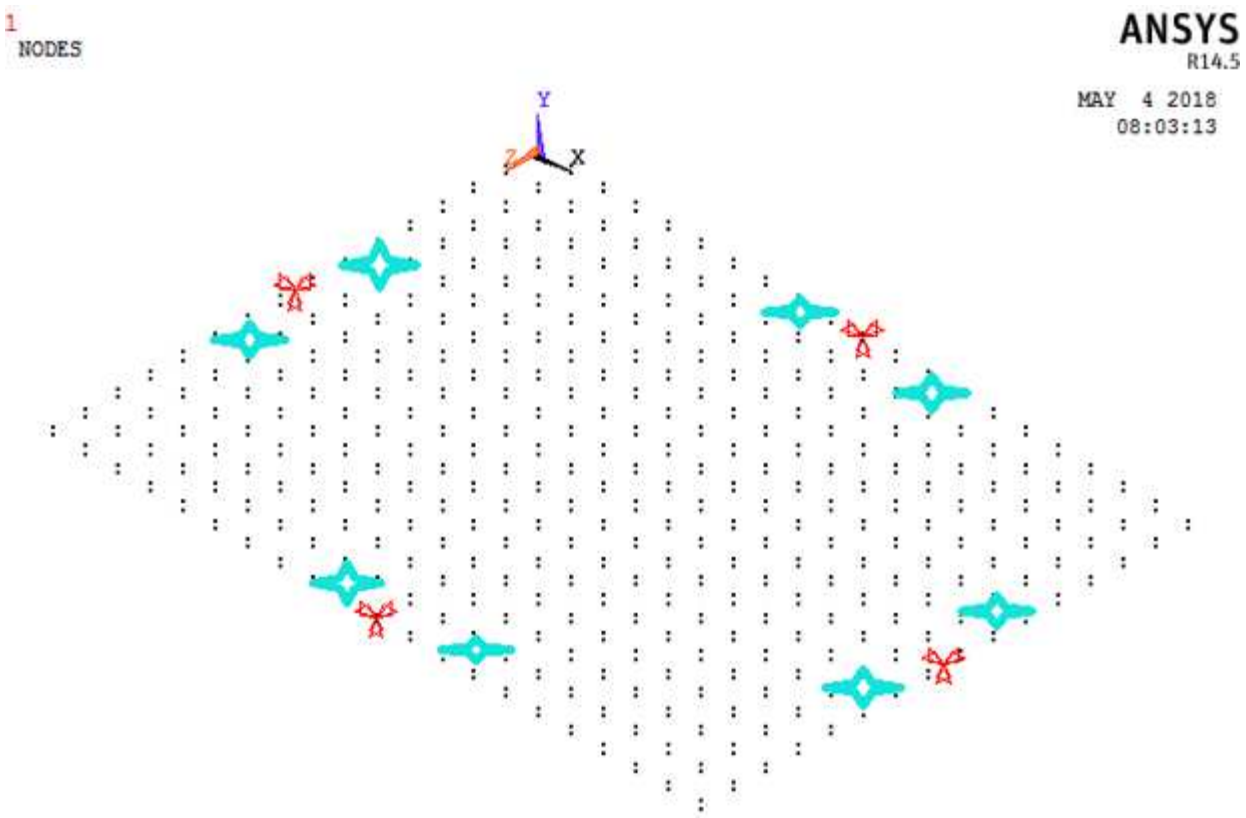

Figure 5.2: Flat plate showing 8 optimum strain gauge locations

5.2.1 Sine wave loading

Before applying an impact load, a repeated sinusoidal load was applied to the flat plate from 0 to 1 seconds. Sinusoidal forcing function F(t)= 8000 sin (30*t) was applied on node 541. The applied load was successfully recovered using CB reduction. The RMS error for reconstruction of the applied load using 1, 5, 10, and 15 retained modes was calculated using Eq. (5.4). The percent root mean square (rms) error showed that as number of modes retained increased, the RMS error gradually decreased. The results corresponding to a use of 1, 5, 10 and 15 retained modes are given in Figs. 5.3-5.6 and Table 5.2.

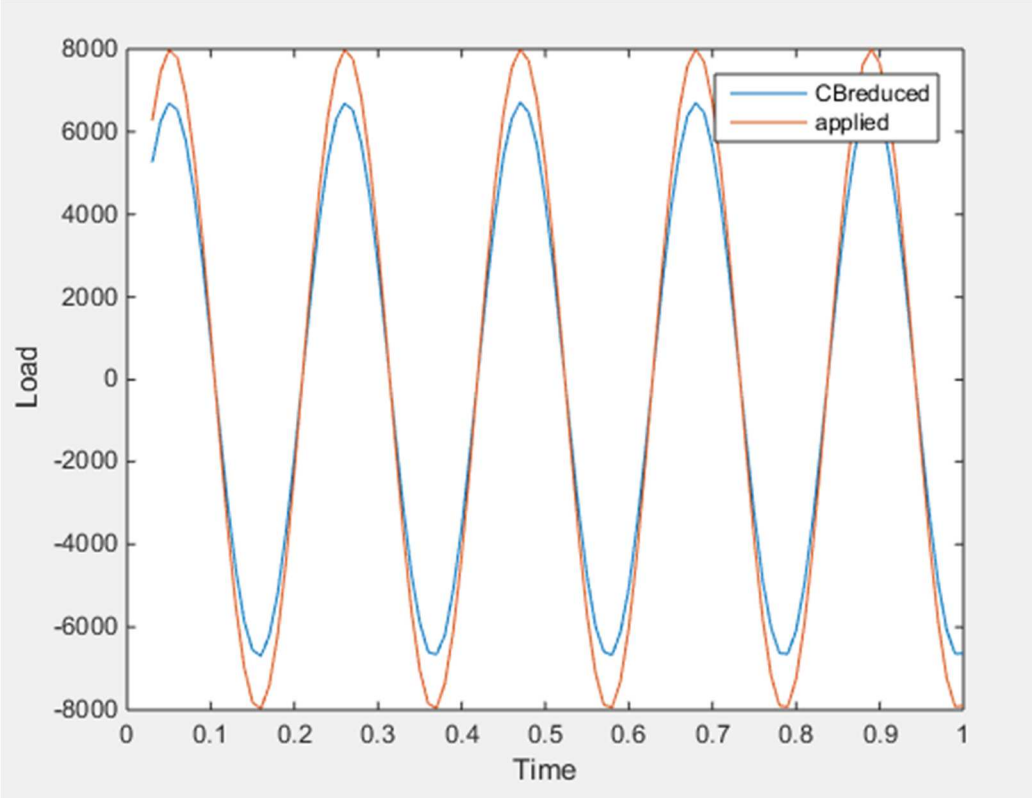

Figure 5.3: Applied load and recovered load using 1 retained mode

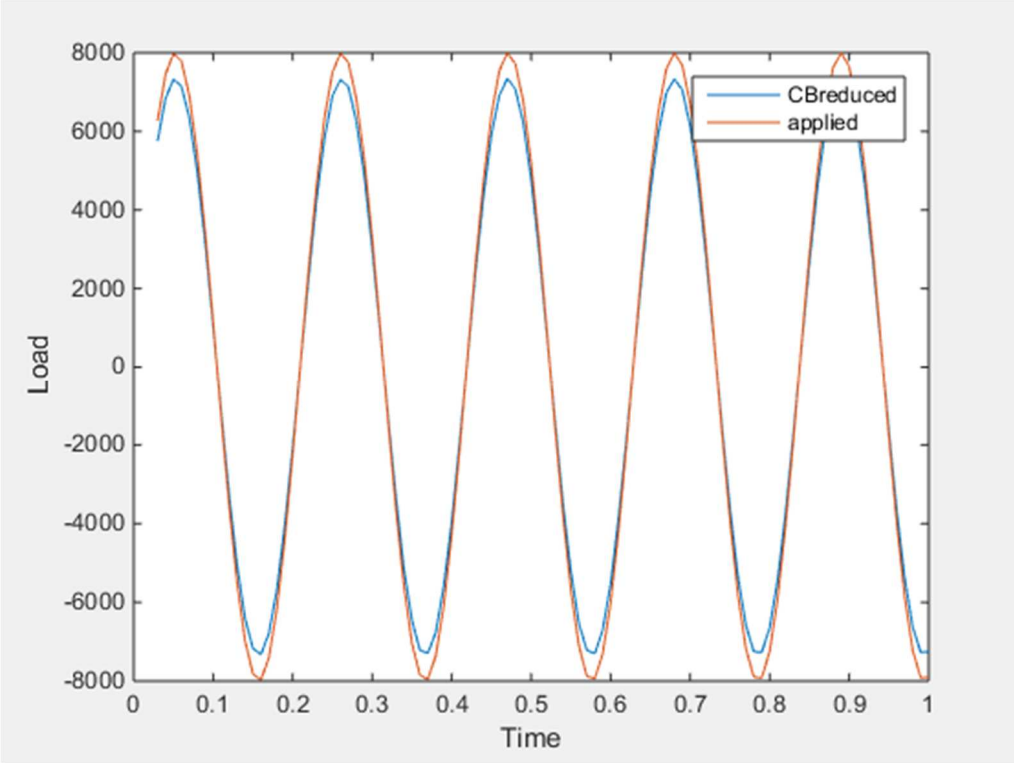

Figure 5.4: Applied load and recovered load using 5 retained modes

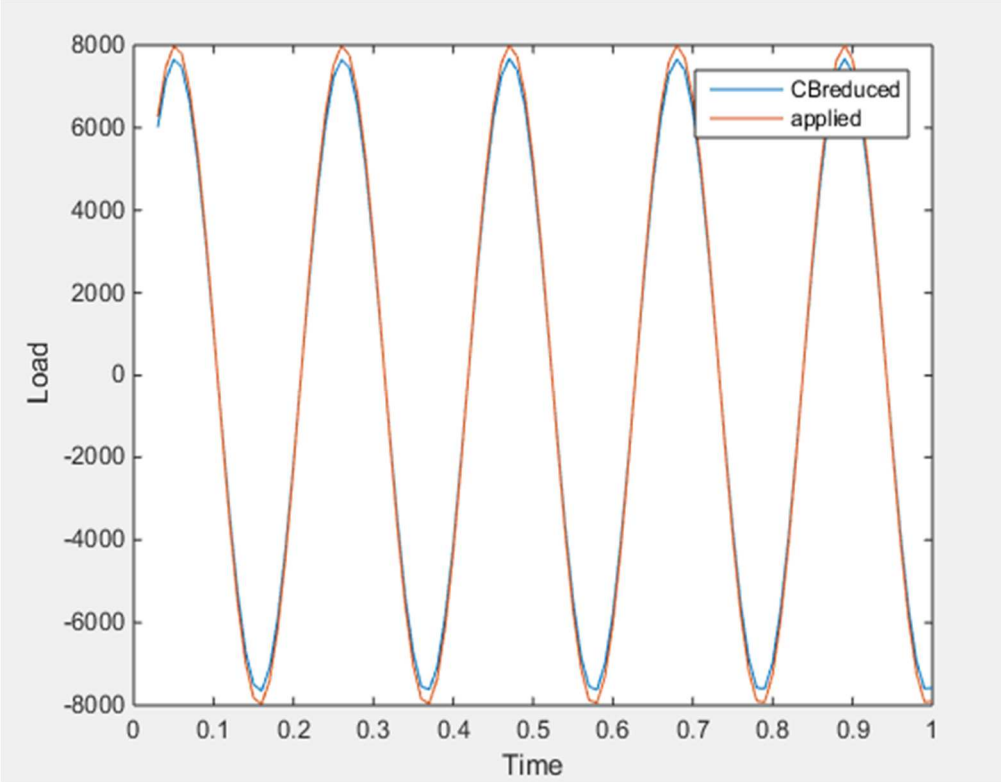

Figure 5.5: Applied load and recovered load using 10 retained modes

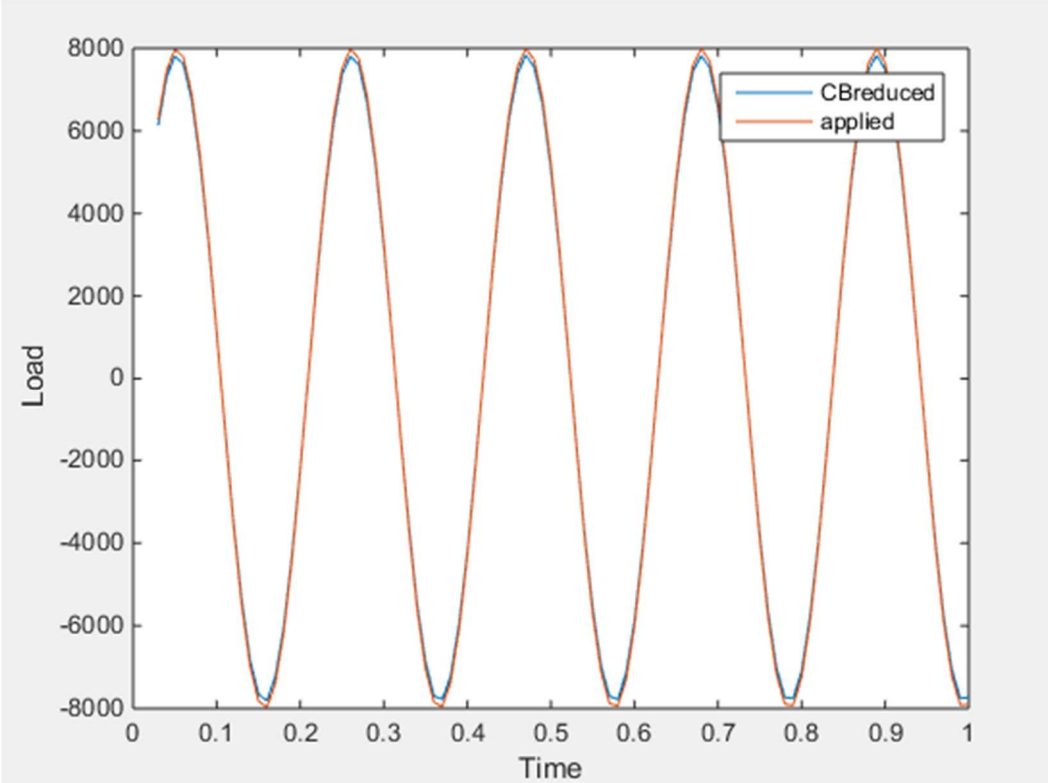

Figure 5.6: Applied and recovered load using 15 retained modes

Table 5.2: Root Mean Square error for different number of retained modes

Number of Retained Modes	RMS error (%)
1	3.27
5	1.66
10	0.82
15	0.42

5.2.2 Triangular Impact loading

Next, triangular impact loading was applied in ANSYS APDL by using KBC, 0 command. The impact load was ramped from 0 N to 8000 N between 0.1 second to 0.2 second. Similarly, impact load was ramped down to 0 N from 0.2 sec to 0.3 second. The impact load was recovered by using Guyan reduction as well as CB reduction. Figure 5.7 presents results for applied load, recovered load without condensation, and recovered loads with Guyan and Craig-Bampton condensations by retaining 7 modes and 8 strain gages.

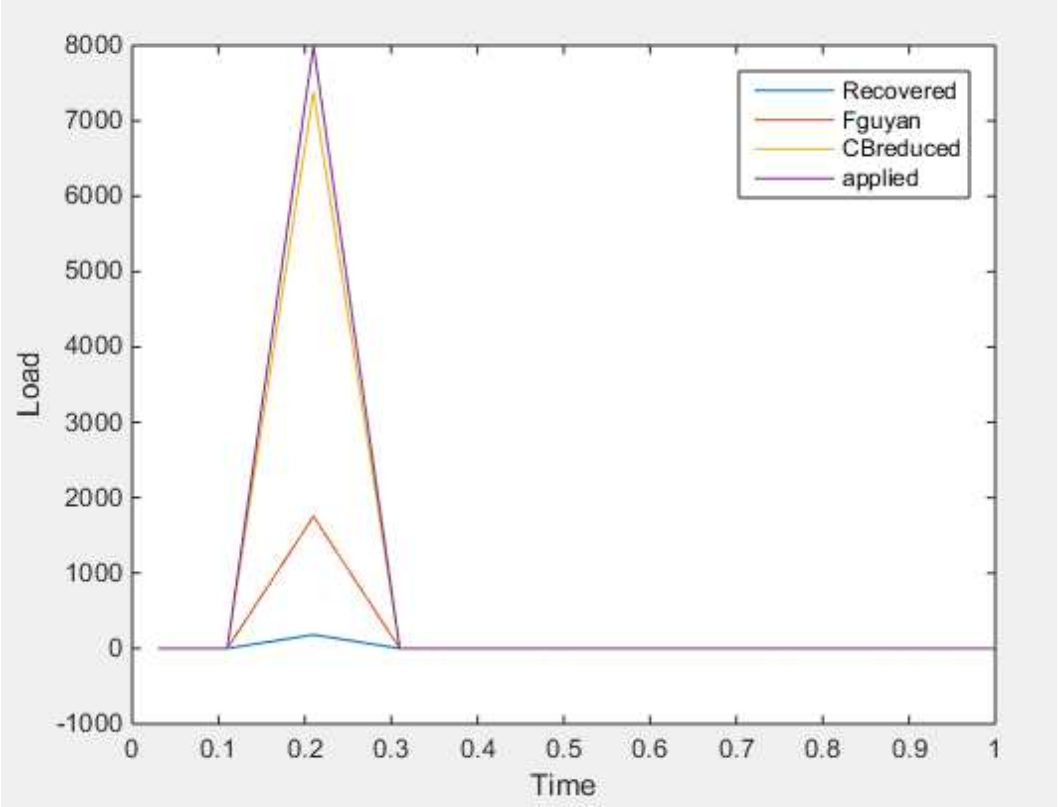

Figure 5.7 : Applied and recovered load using 7 retained modes

5.2.3 Square wave loading

Using steps similar to the triangular impulse load, a square wave loading was applied in ANSYS APDL using KBC, 1 command. The impact load was stepped from 0N to 8000N at 0.1 second and stepped down to 0N at 0.2 seconds. The impact load was recovered CB-reduced model and Guyan Reduction model. Figure 5.8 presents result for applied load, recovered load without condensation, recovered loads with Guyan and Craig-Bampton reduction retaining 15 modes and 17 gages.

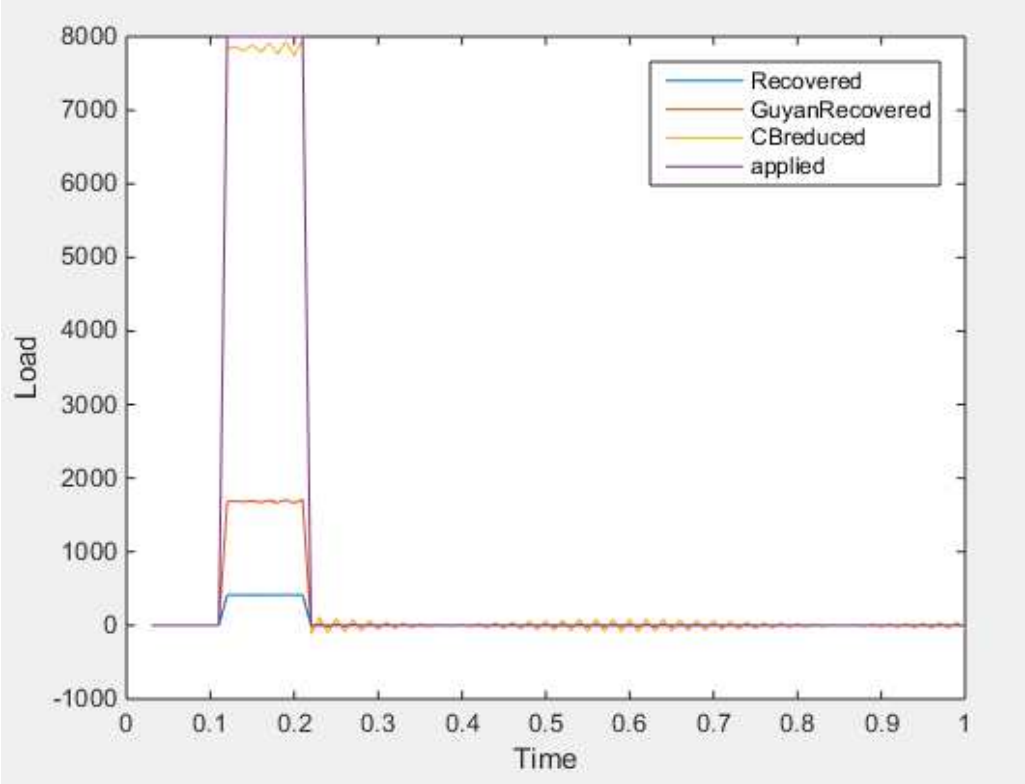

Figure 5.8: Applied and recovered load for a square-wave impact loading using 15 retained modes

5.2.4 Half sine wave loading

Lastly, a half sine wave loading was also applied on the same node of the aluminum plate. A forcing function F= |8000*sin (30t) | was applied to the plate between the interval of 0.1 to 0.314 second to capture half sine loading for 2 cycles. The sinusoidal impact load was recovered using CB reduction and Guyan reduction. Figure 5.9 presents result for applied load, recovered load without condensation, and recovered loads with Guyan and Craig-Bampton condensations retaining 15 modes and 17 gages.

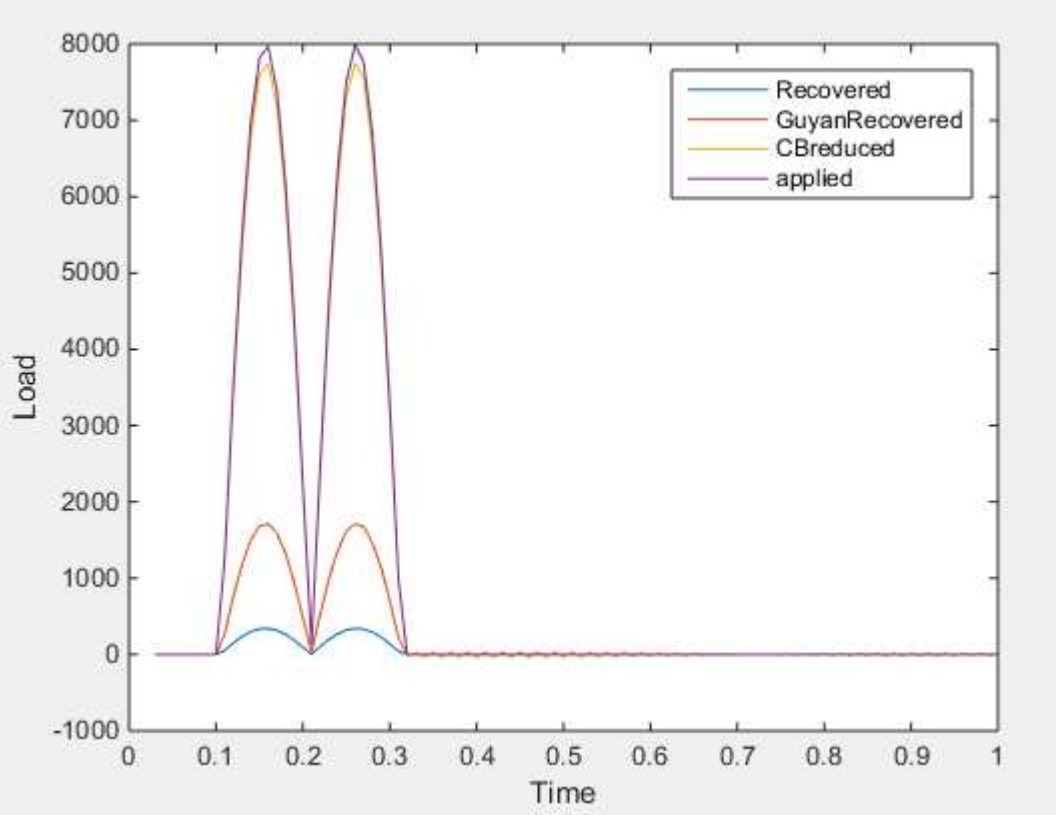

Figure 5.9: Applied and recovered load for half-sine impact loading using 15 retained modes

5.3 Summary

Based on the results presented in Figures 5.7-5.9, it can be seen that the proposed approach based on Craig-Bampton model reduction is effective in capturing the impact loading imposed on the plate. In this chapter, impact loads were recovered on flat plate using strain measurements and model order reduction. The full plate model was reduced using CB-reduction and the three types of impact loading (Triangular wave loading, square wave loading and half-sine wave loading) were applied on certain nodes. Strains, strain mode shapes and displacement mode shapes were extracted at optimum gage locations from ANSYS APDL. The applied impact loads were recovered using CB reduction, Guyan reduction and without using any model reduction. It

is seen that CB reduction technique is most effective in recovering impact loads with a high degree of accuracy.

6 Conclusions and Future Work

6.1 Conclusions

The thesis explains method to recover the impact load by using strains measurements and model order reduction. Reduction techniques like Craig-Bampton reduction and Guyan reduction are extensively used to recover the impact load. The results show that imposed loads could be recovered successfully, using model-order reduction with good accuracy. It is also noted that flat plate with four fixed edges gave more accurate results compared to the 3D cantilever beam that is constrained at one end. One possible reason is that only transverse mode of vibration are present in clamped plate whereas many more modes are excited in 3D cantilever beam. From the results of recovered loads when using 1, 5, 10 and 15 modes, it is seen that the accuracy of load estimates improved as the number of retained mode was increased. It is also noted that use of internal damping improved the numerical stability of results. This was especially true for square-wave impact loads.

6.2 Future Work

The recovery of applied loads was done using Craig Bampton reduction and Guyan reduction. To successfully recover the loads without using reduction technique requires strain data, strain mode shapes and displacement mode shapes at all locations. CB reduction allows us to recover the imposed load with good accuracy using only a small-subset of modal information. However, result of the recovered data varies with the choice of boundary nodes. So, a smart algorithm is required to pick the optimum boundary nodes. Determination of optimum boundary location is also fruitful area of future research.

The thesis addressed impact load acting at only one node. In practical scenario, there might be multiple impact loads applied at different nodes or at the same node. So, recovery of multiple impact loads at different nodes will be a nice extension of the work presented in this thesis.

7 BIBLIOGRAPHY

[1] Augustine, Paul, "Dynamic Moving Load Identification Using Optimal Sensor Placement and Model Reduction" (2015). MS Thesis.

[2] Gupta, Deepak Kumar, "Inverse Methods for Load Identification Augmented By Optimal Sensor Placement and Model Order Reduction" (2013). PhD thesis.

[3] Guyan, R. J. (1965). Reduction of Stiffness and Mass Matrices. *American Institute of Aeronautics and Astronautics (AIAA) Journal, 3* (2), 380.

[4] Craig, R. R., & Bampton, M. C. (1968). Coupling of Substructures for Dynamic Analysis. *American Institute of Aeronautics and Astronautics (AIAA) Journal, 6* (7), 1313-1319.

[5] "Continuous System." *Mechanical Vibrations*, by Singiresu S. Rao, Prentice Hall, 2011, pp. 700–761

[6] ANSYS Mechanical APDL Element Reference, Release 15.0, Help System, Structural Analysis Guide, ANSYS, Inc.

[7] Masroor, S. A., & Zachary, L. W.(1991). Designing an All-Purpose Force Transducer. *Experimental Mechanics*, 31(1), 33-35

[8] Johnson, M.,Nachtsheim, C.J.(1983). Some Guide Lines for Construction Exact D-optimal Designs on Convex Design Spaces, *Technometrics,* Vol.25(3), pp.271-277

[9] Ma, Chih-Kao, et al. "A Study of an Inverse Method for the Estimation of Impulsive Loads." *International Journal of Systems Science*, vol. 29, no. 6, 1998, pp. 663–672.

[10] Khoo, S.y., et al. “Impact Force Identification with Pseudo-Inverse Method on a Lightweight Structure for under-Determined, Even-Determined and over-Determined Cases. *“International Journal of Impact Engineering*, vol. 63, 2014, pp. 52–62.

[11] B. Hillary and D. J. Ewins, The use of strain gauges in force determination and frequency response function measurements, in Proceedings of the 2nd International Modal Ansysyis Conference (IMAC ’84). pp. 627634, Orlando, Fla, USA, 1984.

[12] Wickham, M. J., Riley, D. R., & Nachtsheim, C. J. (1995). Integrating Optimal Experimental Design into the Design of a Multi-Axis Load Transducer. Journal of Engineering for Industry, 117 (3), 400-405.